REMARKS

Claims 1-35, 38-51 and 62-74 are pending. Claims 1-35, 42-49 and 62-74 are withdrawn from consideration. Thus, claims 38-41, 50 and 51 are under examination. Claims 38, 39 and 40 are amended. Support for the amendment to claim 38 can be found in the specification at least at page 13, line 30 to page 14, line 32. Claim 39 was amended for clarity purposes and claim 40 was amended into independent format. No new matter is entered by way of these amendments.

Drawings and Specification Objections

Figure 12a was objected to for being unclear for conflicting with the Brief Description of the Drawings. The Specification on page 6, lines 26-27, in the Brief Description of the Drawings was objected to for being unclear for conflicting with Figure 12a. The specification has been amended to correctly refer to residues 1-346 for chimera VI as shown in Figure 12a. Therefore, Applicants respectfully request withdrawal of these objections.

Claim Objections

Claim 39 was objected to for allegedly lacking a SEQ ID NO in the claim. Applicants respectfully traverse this objection. Claim 39, as amended, recites that the chimera comprises residues 1-314 of NgR1, residues 315-327 of NgR2, and residues 354-473 of NgR1. Claim 39 has been amended for clarity purposes only rather than to limit the claim. Applicants disagree with the Examiner's statement on page 3 of the Office Action that the chimera set forth in claim 39 is SEQ ID NO:21. Claim 39 defines a chimera that contains certain residues of NgR1 and NgR2. Further, Applicants note that claim 39 does not recite any actual amino acids or any specific order of the fragments. Nor does the claim recite that the fragments are juxtaposed. Claim 39 does not require a SEQ ID NO and Applicants respectfully request withdrawal of this rejection.

Claims 39 and 40 were rejected for allegedly being substantial duplicates. As discussed above, the chimera recited by claim 39, as amended, is not the same as SEQ ID NO:21. Therefore, claim 39 differs in scope from claim 40 and Applicants respectfully request withdrawal of this rejection.

Claim 40 was objected to for being dependent upon a rejected base claim. Claim 40 has been amended into independent format and Applicants request withdrawal of this objection and allowance of claim 40.

35 U.S.C. 112, First Paragraph, Enablement

Claims 38, 41, 50 and 51 were rejected for allegedly lacking enablement for NgR1 chimeric proteins comprising a MAG binding motif of NgR2. Although Applicants disagree with the Examiner's assertion that the MAG binding motif is undefined in the specification, claim 38 has been amended to recite a chimeric NgR1 protein comprising residues 315-327 of NgR2 and the ligand binding domain of NgR1. Support for this amendment can be found in the specification at least at page 13, line 30 to page 14, line 32.

Applicants wish to respectfully draw the Examiner's attention to the fact that the allegedly inconsistencies between the specification and Barton et al., *EMBO J.* 22(13):3291-3302 (2003) ("Barton") have been resolved. NgR2 binds MAG. Enclosed is a copy of Venkatesh et al., *The Journal of Neuroscience* 25(4):808-822 (2005) ("Venkatesh"), co-authored by Dr.Giger, one of the Applicants of the present application. Venkatesh states on page 822, right column, second full paragraph, that Barton previously reported NgR2 does not support MAG binding. However, Venkatesh further states that Barton used soluble AP-MAG to test its binding affinity to NgR2. Venkatesh generated AP-MAG and states that, like in Barton, AP-MAG did not bind NgR2. Venkatesh further states that AP tagging of MAG sterically interferes with binding of NgR2 and this accounts for the results of Barton. Also enclosed is a copy of Lauren et al., *Journal of Biological Chemistry* 282(8):5715-5725 (2007) ("Lauren"), showing NgR2 binds MAG. The Examiner's attention is drawn to the fact that both Barton and Lauren were co-authored by Dr. Stephen Strittmatter. On page 5715, Abstract, Lauren states that they have confirmed that MAG binds to NgR2. Therefore, NgR2 binds MAG and the specification is not inconsistent with the art.

Applicants also note that claim 38 is directed to a chimeric NgR1 protein. Thus, data regarding NgR3 chimeric proteins are not relevant to claims 38, 41, 50 and 51.

Claim 38, as amended, recites a chimeric NgR1 protein comprising residues 315-327 of NgR2 and the ligand binding domain of NgR1. As set forth in *Johns Hopkins Univ. v. CellPro Inc.*, 47 USPQ2d 1705, 1714 (Fed. Cir. 1998), "the enablement requirement is met if the

description enables *any* mode of making and using the invention." As pointed out by the Examiner on page 4 of the Office Action, the specification provides several chimeric NgR1 proteins encompassed by claim 38. Thus, the enablement requirement has been met. Specifically, chimeric NgR1 proteins comprising residues 315-327 of NgR2 and the ligand binding domain of NgR1 are described in the specification at least at page 13, line 30 to page 14, line 32. Applicants note that the ligand binding domain of NgR1 is defined at least at page 13, line 30 to page 14, line 32 and Example 5. Nucleic and amino acids sequences of full length NgR1 and NgR2 as well as chimeric NgR1 proteins are described in the specification at least at page 12, line 10 to page 17, line 15. Methods of making chimeric proteins are known and are described in the specification at least at page 48, line 18, to page 55, line 25, including methods of using the full length NgR1 and NgR2 to create a chimeric NgR1 proteins comprising residues 315-327 of NgR2 and the ligand binding domain of NgR1. Methods of using the claimed chimeric proteins are defined by the claims are described in the specification at least at page 43, line 17, to page 57, line 16. Therefore, the specification enables those of skill in the art how to make and use the chimeric NgR1 proteins defined by claims 38, 41, 50 and 51. Applicants respectfully request reconsideration and withdrawal of this enablement rejection.

35 U.S.C. 112, First Paragraph, Written Description

All that is required to satisfy the written description requirement is that the specification provide sufficient description to ***reasonably*** convey to those skilled in the art that, as of the filing date sought, the inventor was in possession of the claimed invention. *Union Oil v. Atlantic Richfield Co.*, 54 U.S.P.Q.2d 1227, 1232 (Fed. Cir. 2000); *Vas-Cath, Inc. v. Mahurkar*, 935 F.2d 1555, 1563-64 (Fed.Cir.1991). Applicants note that the written description requirement does not require a description of the complete structure of every species within a genus. *Utter v. Hiraga*, 6 U.S.P.Q.2d 1709, 1714 (Fed. Cir. 1988). An applicant may show possession of the claimed invention by describing the claimed invention with all of its limitations using such descriptive means as words, structures, figures, diagrams, and formulas that fully set forth the claimed invention. *Lockwood v. American Airlines, Inc.*, 41 USPQ2d 1961, 1966 (Fed. Cir. 1997). Thus the specification need not spell out every detail; only enough "to convince a person of skill in the art that the inventor possessed the invention and to enable such a person to make and use the

invention without undue experimentation." *LizardTech Inc. v. Earth Resource Mapping, Inc.*, 76 USPQ2d 1724, 1732 (Fed. Cir. 2005).

Claim 38, as amended, recites a chimeric NgR1 protein comprising residues 315-327 of NgR2 and the ligand binding domain of NgR1. The specification provides several chimeric NgR1 proteins comprising residues 315-327 of NgR2 and the ligand binding domain of NgR1 at least at page 13, line 30 to page 14, line 32, and Example 5. Applicants note that the ligand binding domain of NgR1 is defined at least at page 13, line 30 to page 14, line 32 and Example 5. One of skill in the art would appreciate that the Applicants were in possession of the chimeric NgR1 proteins defined by claim 38, as amended. Applicants respectfully request reconsideration and withdrawal of this written description rejection based on the claims as amended.

It is believed that all issues raised by the Examiner have been addressed. However, the absence of a reply to a specific rejection, issue, or comment does not signify agreement with or concession of that rejection, issue, or comment. In addition, because the arguments made above may not be exhaustive, there may be reasons for patentability of any or all pending claims (or other claims) that have not been expressed. Finally, the amendment of any claim does not necessarily signify concession of unpatentability of the claim prior to its amendment.

The fee for the Petition for Extension of Time of one-month is being paid concurrently on the Electronic Filing System by way of Deposit Account authorization. Please apply any other charges or credits to deposit account 06-1050.

Respectfully submitted,

Date: April 28, 2008

Tina Williams McKeon
Reg. No. 43,791

1180 Peachtree Street, N.E., 21st Floor
Atlanta, GA 30309
Telephone: (404) 892-5005
Facsimile: (404) 892-5002

Development/Plasticity/Repair

The Nogo-66 Receptor Homolog NgR2 Is a Sialic Acid-Dependent Receptor Selective for Myelin-Associated Glycoprotein

Karthik Venkatesh,[1] Onanong Chivatakarn,[1] Hakjoo Lee,[1] Pushkar S. Joshi,[1] David B. Kantor,[2] Barbara A. Newman,[3] Rose Mage,[3] Christoph Rader,[4] and Roman J. Giger[1]

[1]Center for Aging and Developmental Biology, University of Rochester School of Medicine and Dentistry, Rochester, New York 14642, [2]Department of Neuroscience, The Johns Hopkins University School of Medicine, Baltimore, Maryland 21205, [3]Laboratory of Immunology, National Institute of Allergy and Infectious Diseases, National Institutes of Health, Bethesda, Maryland 20892-1892, and [4]Experimental Transplantation and Immunology Branch, Center for Cancer Research, National Cancer Institute, National Institutes of Health, Bethesda, Maryland 20892-1907

The Nogo-66 receptor (NgR1) is a promiscuous receptor for the myelin inhibitory proteins Nogo/Nogo-66, myelin-associated glycoprotein (MAG), and oligodendrocyte myelin glycoprotein (OMgp). NgR1, an axonal glycoprotein, is the founding member of a protein family composed of the structurally related molecules NgR1, NgR2, and NgR3. Here we show that NgR2 is a novel receptor for MAG and acts selectively to mediate MAG inhibitory responses. MAG binds NgR2 directly and with greater affinity than NgR1. In neurons NgR1 and NgR2 support MAG binding in a sialic acid-dependent *Vibrio cholerae* neuraminidase-sensitive manner. Forced expression of NgR2 is sufficient to impart MAG inhibition to neonatal sensory neurons. Soluble NgR2 has MAG antagonistic capacity and promotes neuronal growth on MAG and CNS myelin substrate *in vitro*. Structural studies have revealed that the NgR2 leucine-rich repeat cluster and the NgR2 "unique" domain are necessary for high-affinity MAG binding. Consistent with its role as a neuronal MAG receptor, NgR2 is an axon-associated glycoprotein. In postnatal brain NgR1 and NgR2 are strongly enriched in Triton X-100-insoluble lipid rafts. Neural expression studies of NgR1 and NgR2 have revealed broad and overlapping, yet distinct, distribution in the mature CNS. Taken together, our studies identify NgRs as a family of receptors (or components of receptors) for myelin inhibitors and provide insights into how interactions between MAG and members of the Nogo receptor family function to coordinate myelin inhibitory responses.

Key words: neuron; axon; neurite outgrowth; myelin; MAG; Nogo receptor; ganglioside

Introduction

In higher vertebrates, including humans, the regenerative capacity of injured CNS neurons is extremely limited. Multiple lines of evidence point to CNS myelin as a major source for inhibitory proteins that impair axonal regeneration (Schwab et al., 1993; McGee and Strittmatter, 2003). One of the best characterized inhibitors of axonal growth is myelin-associated glycoprotein (MAG) (Filbin, 2003). *In vitro*, MAG regulates neurite outgrowth in an age-dependent manner. MAG promotes growth of many types of embryonic and neonate neurons and, at more mature stages, strongly inhibits growth (Johnson et al., 1989; McKerracher et al., 1994; Mukhopadhyay et al., 1994; Hasegawa et al., 2004). Loss of MAG is not sufficient to improve regenerative growth in spinal cord-injured mice (Bartsch et al., 1995), but there is good evidence that MAG has growth inhibitory activity toward regenerating neurons *in vivo* (Schafer et al., 1996; Sicotte et al., 2003).

MAG, a sialic acid-binding Ig-like lectin (Siglec), binds preferentially to carbohydrates bearing terminal α2,3-linked sialic acids (Crocker and Varki, 2001; Vyas and Schnaar, 2001). MAG binds to the neuronal cell surface and inhibits growth in a sialic acid-dependent *Vibrio cholerae* neuraminidase-sensitive (VCN-sensitive) manner (Kelm et al., 1994; DeBellard et al., 1996). Select gangliosides, including GT1b and GD1a, support sialic acid-dependent MAG binding and play an important role in MAG inhibitory neuronal responses (Yang et al., 1996; Vinson et al., 2001; Vyas et al., 2002). However, the mechanisms of how MAG binding to gangliosides triggers intracellular signaling events, such as activation of RhoA, are not well understood. The sialic acid dependence of MAG inhibition was challenged by the recent identification of the Nogo-66 receptor (NgR1) as a high-affinity MAG receptor that supports binding in a sialic acid-independent manner (Domeniconi et al., 2002; Liu et al., 2002). The MAG–NgR1 interaction is functionally significant; anti-NgR1 antibod-

Received Aug. 29, 2004; revised Nov. 30, 2004; accepted Dec. 2, 2004.

This work was supported by the New York State Spinal Cord Injury Research Program (R.J.G. and C.R.), the Ellison Medical Foundation, National Alliance for Research on Schizophrenia and Depression, the Alexandrine and Alexander Sinsheimer Foundation, National Institute of Neurological Disorders and Stroke Grant NS047333 (R.J.G.), and National Institutes of Health Training Grant T32 NS07489 (K.V.). We thank J. Lee-Osbourne, D. Welch, M. Lefort, and T. Wychowski for excellent technical assistance; Z. Ali for anti-NgR1 and anti-NgR2 tissue Western blots; A. Kolodkin for NgR1 and NgR2 expression plasmids; R. Schnaar for MAG-Fc, CHO-MAG, and CHO-R2 cell lines; M. Filbin for MAG-Fc; Z. He for AP-OMgp; H. Federoff for Ad-RFP; and M. Lefort for help with figures.

Correspondence should be addressed to Roman J. Giger, Graduate Program in Neuroscience, Center for Aging and Developmental Biology, University of Rochester School of Medicine and Dentistry, 601 Elmwood Avenue, Rochester, NY 14642. E-mail: Roman_Giger@URMC.Rochester.edu.

DOI:10.1523/JNEUROSCI.4464-04.2005

 0270-6474/05/250808-15$15.00/0

ies block MAG inhibition (Domeniconi et al., 2002; Li et al., 2004), and ectopic expression of NgR1 in embryonic chick dorsal root ganglion (DRG) neurons is sufficient to confer MAG responsiveness (Liu et al., 2002).

Based on initial observations that neurons from *p75* mutant mice are no longer inhibited by MAG (Yamashita et al., 2002), two subsequent studies identified the pan-neurotrophin receptor p75 as the signal-transducing component in a NgR1/p75 receptor complex (K. C. Wang et al., 2002b; Wong et al., 2002). In addition, Lingo-1/Lern-1, a nervous system-specific type-I membrane protein (Carim-Todd et al., 2003), is an essential component of the NgR1/p75 receptor system *in vitro* (Mi et al., 2004). In spinal cord-injured mice, however, depletion of functional p75 is not sufficient to improve the regenerative growth of descending corticospinal or ascending sensory neurons (Song et al., 2004). This implies the existence of p75-independent mechanisms sufficient to bring about inhibition *in vivo*.

The recent identification of NgR2 and NgR3, two NgR1-related proteins, raises the question as to whether these molecules, similar to NgR1, play a role in myelin inhibition. Here we report the identification of NgR2 as a high-affinity and sialic acid-dependent receptor for MAG.

Materials and Methods

Reagents. The following materials were used: OptiMEM, DMEM, Neurobasal medium, L15, B27 supplement, fetal bovine serum (FBS), dialyzed FBS, HBSS, Pen/Strep, G418, and glutamine (Invitrogen, San Diego, CA); MAG-Fc (M. Filbin, Hunter College, City University of New York, New York, NY; R. Schnaar, Johns Hopkins University, Baltimore, MD; and R & D Systems, Minneapolis, MN); CHO-MAG and CHO-R2 cells (R. Schnaar); oligodendrocyte myelin glycoprotein (OMgp-AP; Z. He, Children's Hospital, Harvard Medical School, Boston, MA); Siglec 3-Fc and NgR-Fc (R & D Systems); Ad-RFP (H. Federoff, University of Rochester, Rochester, NY); anti-caveolin (Upstate Biotechnology, Lake Placid, NY); anti-human Fc-AP-conjugated, anti-rabbit IgG-AP-conjugated, class III β-tubulin antibody (Tuj1; Promega, Madison, WI); anti-MAG monoclonal antibody 513 (mAb 513) and anti-p75 clone 192 (Chemicon, Temecula, CA); Alexa red anti-mouse IgG and Alexa green anti-rabbit IgG (Molecular Probes, Eugene, OR); anti-green fluorescent protein (anti-GFP; Rockland Immunochemicals, Gilbertsville, PA); anti-AP (American Research Products, Belmont, MA); anti-myc (9B11; Cell Signaling Technology, Beverly, MA); spin columns (Vivascience, Edgewood, NY); VCN, RNA polymerases, Tth-DNA polymerase, and DIG-RNA labeling kit (Roche Molecular Biochemicals, Indianapolis, IN); isopropyl β-D-thiogalactoside (IPTG), Lipofectamine 2000, and pTrcHis (Invitrogen); Percoll (MP Biomedicals, Irvine, CA); mammalian tissue protease inhibitor mixture, insulin, transferrin, NBT/BCIP tablets, T3/T4, progesterone, MES, and selenium (Sigma, St. Louis, MO); restriction enzymes (New England Biolabs, Beverly, MA); Protein G Plus/Protein A-agarose beads (Oncogene, San Diego, CA); BCA kit (Pierce, Rockford, IL); HRP/ECL detection system (Amersham Biosciences, Piscataway, NJ); and ABC system (Vector Laboratories, Burlingame, CA).

Identification of NgR2 and NgR3. tBLAST database searches with full-length NgR1 revealed several human and mouse expressed sequence tags (ESTs) with identities between 41 and 63% to NgR1. EST (Gi42742490) was used to generate primers for RT-PCR. Primers 207-forward GCCATCCCGGAGGGCATCCC and 207-back ACACTTATAGAGGTAGAGGGCGTG amplified a 267 bp PCR product from embryonic day 15 (E15) rat brain first-strand cDNA. The EST clone IMAGE:1926673 (GenBank accession number AI346757) was ordered from Genome Systems (St. Louis, MO). Both cDNA fragments were labeled with ^{32}P-dCTP and used to screen an E15 rat spinal cord/DRG cDNA library (Kolodkin et al., 1997). Several clones were identified and endsequenced. Of these, clones 207-17 (2.1 kb) and 208-56 (1.9 kb) contained the largest inserts and were sequenced on both strands, revealing open reading frames of the NgR1-like polypeptides NgR2 and NgR3.

Generation of immune sera. Rabbits were immunized with 6-his-tagged fusion proteins of each of the NgR family members. Fusion proteins include the less-conserved C-terminal sequences: the LRRCT and the "unique" domains of NgR1 (amino acids 278–473), NgR2 (amino acids 279–420), and NgR3 (amino acids 274–445). Fusion proteins were expressed from the pTrcHis vector after induction with IPTG (1 mM) of *Escherichia coli* cultures at an OD_{600} of 0.8. The three 6-his-tagged fusion proteins were purified over a Ni-NTA column and used for rabbit immunization (Popkov et al., 2003).

Generation of ligand and receptor constructs. Human placental alkaline phosphatase-tagged (AP-tagged) fusion proteins were constructed by standard PCR cloning techniques, using the Tth-DNA polymerase and assembled in the pcDNA-AP vector after digestion with *Bgl*II and *Eco*R1 (Giger et al., 1998). AP-Nogo-66 (Fournier et al., 2001), AP-NiG (Niederost et al., 2002), OMgp-AP (Wang et al., 2002a), AP-Fc (Giger et al., 1998), AP-MAG (Liu et al., 2002), AP-sNgR1 (Ala^{24}–Glu^{445}), AP-sNgR2 (Ser^{30}–Ser^{396}), and AP-sNgR3 (Ser^{22}–Val^{420}) were expressed in Lipofectamine 2000-transfected HEK293T cells and harvested from conditioned cell culture supernatant in OptiMEM. Expression of fusion proteins was confirmed by immunoblotting with anti-AP serum. For ligand quantification the AP activity was determined enzymatically (OD_{405}). If necessary, ligands were concentrated by using spin columns with a molecular weight cutoff of 10 kDa. Receptor constructs included N-terminally myc-tagged NgR1(Pro^{26}–Cys^{473}), myc-NgR2 (Ser^{30}–Leu^{420}), and myc-NgR3 (Gly^{24}–Arg^{445}) assembled in the expression vector pMT21 (Kolodkin et al., 1997). Also included were chimera NgR2^{LRR}(Met^{1}–Pro^{313})/NgR1^{unique}(Gly^{314}–Cys^{473}) fused by *Spe*I, introducing Thr^{314} and Ser^{315}; NgR1^{LRR}(Met^{1}–Val^{311})/NgR2^{unique}(Pro^{315}–Lys^{420}) fused by *Spe*I, introducing Thr^{312} and Ser^{313}; NgR3^{LRR}(Met^{1}–Pro^{307})/NgR2^{unique}(Pro^{315}–Lys^{420}) fused by *Spe*I, introducing Thr^{308} and Ser^{309}; NgR1$^{\Delta unique}$(Met^{1}–Pro^{312})/NgR1(Leu^{431}–Cys^{473}) fused by *Spe*I/*Xba*I, introducing Thr and Arg at the fusion site; NgR2$^{\Delta unique}$(Met^{1}–Val^{311})/NgR1(Leu^{431}–Cys^{473}) fused by *Spe*I/*Xba*I. For adenoviral vectors the full-length NgR1 and NgR2 were cloned into pAdTrack-CMV and recombined with pAdEasy-1 in *E. coli*. Recombinant virus was produced and amplified in HEK293 cells and purified by double CsCl banding as described previously (Giger et al., 1997).

Ligand–receptor binding studies. Receptor constructs were expressed transiently in COS-7 cells in 24-well plates coated with poly-D-lysine (PDL; 50 μg/ml), using Lipofectamine 2000. To assess cell surface expression of transiently expressed receptor constructs, we stained some wells with anti-NgR1 (1:1000), anti-NgR2 (1:1000), or anti-NgR3 (1:200) under nonpermeabilizing conditions. At 24 h after transfection the cells were rinsed and incubated for 75 min at ambient temperature with the following (in nM): 10 AP-Nogo-66, 10 OMgp-AP, 20 AP-NiG, 20 AP-Fc, 33 AP-MAG, 17 MAG-Fc, 30 Siglec 3-Fc, or 8 anti-human Fc-AP-conjugated antibody. Before binding, MAG-Fc and Siglec 3-Fc were oligomerized by preincubation with anti-human Fc conjugated to AP (2:1). Of note, dimeric MAG-Fc (not preclustered by preincubation with anti-human Fc-AP) still binds to NgR2 in COS-7 cells (see Fig. 2*B*). Consistent with previous studies, however, the strength of binding is increased if MAG-Fc is oligomerized (Strenge et al., 1999). For antibody blocking of MAG binding the MAG-Fc was preincubated for 1 h with anti-MAG mAb 513 (10 μg/ml) or anti-p75 mAb 192 (10 μg/ml) in OptiMEM. Unbound ligand was removed by several rinses in HBHA (1× HBS supplemented with 20 mM HEPES, pH 7.0, 0.05% BSA, 0.5% NaN_3). Cells were fixed in 60% acetone, 1% formaldehyde, and 20 mM HEPES, pH 7.0, rinsed in HBHA, and heated at 65°C in HBS for 60 min. To monitor bound ligand, we developed plates with NBT/BCIP substrate; the color reaction was stopped by two rinses in PBS. For quantification of ligand binding the cells were processed as described above; after ligand incubation the cells were rinsed in HBHA and lysed in 20 mM Tris, pH 8.0, 0.1% Triton X-100. The lysates were incubated at 65°C for 60 min and spun at 10,000 × *g* for 5 min. The relative AP activity in supernatants was normalized to cell surface receptor expression, using anti-myc (1:1000), anti-NgR1 (1:1000), anti-NgR2 (1:1000), or anti-NgR3 (1:200) antibodies, as described previously (Giger et al., 1998). Scatchard plot analysis of the MAG-Fc binding to NgR2-expressing COS-7 cells was performed analogous to a previous study (Kolodkin et al., 1997). For binding of MAG-Fc and AP-Nogo-66 to dissociated DRGs 25,000 cells/well were

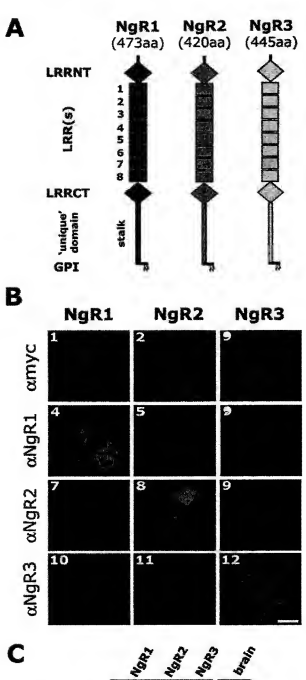

Figure 1. Characterization of antibodies raised against Nogo receptor family members. *A*, Domain alignment of the Nogo receptor family members NgR1 (473 amino acid residues), NgR2 (420 amino acid residues), and NgR3 (445 amino acid residues). Nogo receptors are composed of eight canonical leucine-rich repeats (LRR1–LRR8) flanked by cysteine-rich LRRNT and LRRCT subdomains. The highly conserved LRRNT+LRR+LRRCT domains are connected via a more variable unique domain (stalk) to a GPI anchor for membrane attachment. We raised polyclonal antibodies against the distal part of the LRRCT and the unique domain of each of the three NgR family members. *B*, Immunocytochemistry (ICC) under nonpermeabilizing conditions of myc-tagged NgR1, NgR2, and NgR3 in transfected COS-7 cells reveals abundant cell surface localization of NgR1 (*B1*), NgR2 (*B2*), and NgR3 (*B3*). Anti-NgR1 (*B4*), anti-NgR2 (*B8*), and anti-NgR3 (*B12*) immune sera strongly and selectively react with their cognate antigens. No cross-reactivity with other NgR family members is observed. *C*, Western blotting with anti-NgR1, anti-NgR2, and anti-NgR3 immune sera allows for selective detection of recombinant (COS-7) and endogenously (adult rat brain) expressed receptors. All three NgR family members are expressed abundantly in the adult brain. Of note, endogenously expressed NgR1 and NgR2 are detected as single bands and migrate at an apparent molecular weight of 65 kDa. Recombinant NgR1 and NgR2 occur as multiple variants between 55 and 70 kDa (Walmsley et al., 2004). Multiple variants are found for recombinant and endogenously expressed NgR3. Scale bar, 20 μm.

plated in four-well plates on 100 μg/ml PDL and cultured in Sato$^+$ medium [20 nM progesterone, 30 nM selenium, 5 μg/ml insulin, 4 mg/ml BSA, 0.1 μg/ml L-thyroxine, 0.08 μg/ml triiodo-thyronine; for neonatal (postnatal day 1–2 [P1–P2]) DRGs 15 ng/ml NGF was added]. After 48 h the DRGs were infected with adenoviral NgR1 (Ad-NgR1) or Ad-NgR2 (multiplicity of infection, ~100). Before ligand-binding studies the viral transduction of DRGs was confirmed by live monitoring of GFP expression. Then neuronal cultures were rinsed and incubated in OptiMEM or OptiMEM with VCN (20 mU/ml) at 37°C for 1 h. Ligand binding was performed as described above.

Histochemical procedures. For *in situ* hybridization cryosections of postnatal rat tissue were incubated with digoxigenin-labeled (DIG-11-UTP; Roche Molecular Biochemicals) cRNA probes generated by *in vitro* transcription, using the T3, T7, or SP6 RNA-polymerase. Probes for *NgR1* and *NgR2* were transcribed from cDNA fragments encoding the less-conserved C-terminal sequences and included a *NgR1* (0.96 kb fragment in pGEM downstream of codon Arg^{279}) linearized with *Xho*I or *Xba*I to generate sense (T7) and antisense (SP6) probes and a *NgR2* (1.03 kb fragment in pBluescript downstream of codon Arg^{280}) linearized with *Xba*I or *Eco*R1 to generate sense (T3) and antisense (T7) probes. In addition, a DIG-labeled VIP sense probe was used as a negative control. To enhance tissue penetration, we carbonate-digested cRNA probes at 60°C, pH ~11, for 45 min, to an average length of 150–250 bases. Hybridization was performed at 60°C in 50% formamide, with a final concentration of ~100–200 ng of DIG probe/ml hybridization solution (Giger et al., 1996).

For immunohistochemistry the eyes of adult rats were flash frozen in dry ice-cooled isopentane and cryosectioned at 20 μm. Sections were fixed for 10 min in cooled methanol, followed by several rinses in PBS. Endogenous peroxidases were quenched; sections were blocked in normal goat serum and incubated in primary antibody overnight at 4°C. Anti-NgR1 (1:1000) and anti-NgR2 (1:1000) were detected with a biotinylated anti-rabbit IgG (1:500) and visualized by using the Ni-enhanced horseradish peroxidase ABC system. Sections were dehydrated in a graded series of ethanol and cleared in xylene.

Isolation of lipid rafts and immunoblotting. Brains obtained from P14 rats were homogenized in ice-cold MES-buffered saline containing 0.1% Triton X-100 and protease inhibitor mixture. The homogenate was passed several times through a 21-gauge needle, and cellular debris was removed by low speed centrifugation (3000 × *g* for 15 min). From the resulting supernatant Triton X-100-insoluble membrane rafts were enriched by flotation in a 5–40% sucrose gradient for 36 h at 200,000 × *g*. Fractions of the gradient were collected (0.5 ml), diluted in PBS, and precipitated at 10,000 × *g* for 30 min. Pellets were resuspended and subjected to Western blot analysis by using anti-NgR1 (1:2000), anti-NgR2 (1:2000), or anti-caveolin (1:1000) antibodies. Fractions containing the highest amounts of NgR1 and NgR2 were pooled and incubated in OptiMEM or OptiMEM and VCN (20 mU/ml) at 37°C for 1 h before Western blot analysis.

Affinity precipitation. COS-7 cells in 10 cm culture dishes were infected with Ad-NgR1 or Ad-NgR2 in OptiMEM. After 24 h the cells were incubated in lysis buffer containing the following (in mM): 20 Tris-HCl, pH

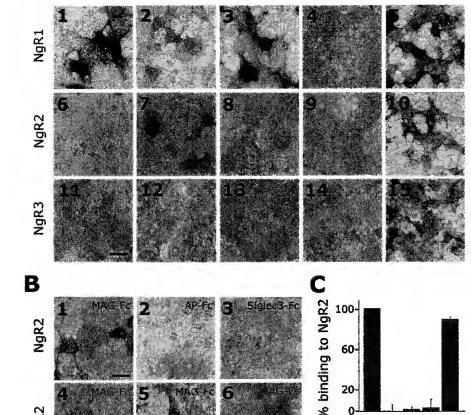

Figure 2. Binding profile of myelin inhibitors to Nogo receptors. *A*, Binding of AP-Nogo-66 (*A1*, *A6*, *A11*), MAG-Fc (*A2*, *A7*, *A12*), OMgp-AP (*A3*, *A8*, *A13*), and AP-NiG (*A4*, *A9*, *A14*) to recombinant NgR1, NgR2, and NgR3 transiently expressed in COS-7 cells. Bound MAG-Fc was detected with anti-human Fc conjugated to AP. Immunocytochemistry with anti-NgR1 (*A5*), anti-NgR2 (*A10*), and anti-NgR3 (*A15*) was used to confirm expression of transfected receptor constructs. *B*, NgR2 supports binding of oligomerized MAG-Fc (*B1*), but not AP-Fc (*B2*) or Siglec3-Fc (*B3*). Binding of oligomerized MAG-Fc to NgR2 is blocked by anti-MAG 513 (*B4*), but not by anti-p75 192 IgG (*B5*). MAG-Fc that has not been oligomerized with anti-human Fc (unclustered) still binds to NgR2 (*B6*). *C*, Quantification of ligand binding in relative AP units. Binding of MAG to NgR2 is equal to 100%. NgR2 does not support AP-Fc or Siglec3-Fc binding. MAG binding is blocked in the presence of anti-MAG (10 μg/ml), but not anti-p75 (10 μg/ml) IgG. Scale bars: *A*, *B*, 20 μm.

7.5, 150 NaCl, 5 EDTA plus 1% NP-40 and protease inhibitor mixture. Cell lysates were tumbled overnight at 4°C in the presence of MAG-Fc (2 μg) or control IgG (2 μg) and precipitated with Protein G Plus/Protein A-agarose after incubation at 4°C for 2 h. Cell lysates of Ad-NgR2-transduced COS-7 cells, AP-Nogo-66 (15 nM), or AP-NiG (20 nM) were incubated with NgR-Fc (2 μg) and precipitated with Protein G Plus/Protein A-agarose after incubation at 4°C for 2 h. To assess direct MAG interactions, we preincubated 1 nM AP-sNgR1, 1 nM AP-sNgR2, or 1 nM AP-sNgR3 in OptiMEM with 1 μg of MAG-Fc. Precipitated beads were rinsed three times with lysis buffer, and bound proteins were eluted with 2× SDS sample buffer. Precipitates were analyzed by immunoblotting, using anti-NgR1, anti-NgR2, or anti-AP antisera.

For affinity precipitation studies with neurons the cultures of P1–P2 DRGs were transfected with Ad-NgR1 and Ad-NgR2 as described above. To remove terminal sialic acids, we incubated the cultures for 1 h in VCN (20 mU/ml at 37°C). Lysis and affinity precipitation with MAG-Fc (2 μg), AP-Nogo-66 (1 μg), or control IgG (2 μg) were performed as described above.

Neurite outgrowth assays. CHO-MAG cells were FACS-sorted (FACS Vantage SE), using anti-MAG mAb 513 (1 μg/10^6 cells). Briefly, CHO-MAG cells were detached from culture plates with trypsin, rinsed in DMEM/10% FBS, incubated in primary antibody for 15 min at room temperature, rinsed in DMEM/10% FBS, and incubated in secondary antibody (2 μg/10^6 cells) for 25 min (anti-mouse Alexa red). The top 20% of sorted cells was selected, resulting in a cell population expressing homogenous and high levels of MAG. Cell surface expression of MAG was confirmed by anti-MAG (mAb 513) immunocytochemistry under nonpermeabilizing conditions. Control CHO and CHO-MAG cells were cultured in DMEM, 10% dialyzed FBS, 2 mM glutamine, 40 mg/L proline, 0.73 mg/L thymidine, 7.5 mg/L glycine (and 400 μg/ml G418 for CHO-MAG). For feeder layers 300,000 cells/well were seeded in PDL-coated (50 μg/ml) four-well plates and cultured overnight. DRGs were dissected from neonate (P1 or P2) pups and adult rats, incubated in 0.05% trypsin and 0.1% collagenase, triturated, and cultured in Sato$^+$ supplemented with 15 ng/ml NGF (for neonatal DRGs only) at a density of 2 × 10^5 cells/well. Adenoviral infection (Ad-NgR1, Ad-NgR2, and Ad-RFP; multiplicity of infection, ~100) of DRGs was performed for 3–6 h in PDL-coated four-well plates. After viral transfection the DRGs were detached gently from culture plates, rinsed in Neurobasal medium, transferred onto CHO or CHO-MAG feeder layers, and cultured in Sato$^+$ for 18–20 h.

Cerebellar granule neurons (CGNs) from P7 rat pups were purified in a discontinuous Percoll gradient (Hatten, 1985). CGNs at the 35/60% Percoll interface were collected, rinsed, and cultured in Neurobasal medium with 1× B27 supplement, 25 mM glucose, 1 mM glutamine, and Pen/Strep. For transfection of CGNs the Amaxa Biosystems (Köln, Germany) nucleofection technology was used. Briefly, 5–7 × 10^6 CGNs in 100 μl of Nucleofector kit V solution were mixed with 3 μg of pEGFP-N1 plasmid DNA or a mixture of 3 μg of pMT21-NgR2 and 1 μg of pEGFP-N1 plasmid DNA and transferred into a cuvette for electroporation. Cells were transfected by using the O-03 pulsing parameter, transferred into 0.5 ml of 37°C prewarmed Neurobasal medium containing 10% FBS, and incubated for 30 min at 37°C. Cells were rinsed once in culture medium and plated on monolayers of CHO or CHO-MAG cells in six-well plates for 20 h at a density of 1 million per well.

For neurite outgrowth on MAG spots the MAG-containing substrata were prepared from either CHO-MAG cells or adult rat spinal cord as described (Vyas et al., 2002). Briefly, CHO-MAG cells from 10 confluent 10 cm plates or adult rat spinal cord tissue were homogenized in ice-cold 0.32 M sucrose, 50 mM HEPES, 1 mM DTT, and protease inhibitor. Membranes were isolated in a sucrose gradient, followed by two osmotic shocks (Norton and Poduslo, 1973). Recombinant MAG from CHO-MAG cell membranes was extracted in 60 mM 3-[(3-cholamidopropyl) dimethylammonio]-1-propanesulfonate (CHAPS). Endogenous MAG from adult rat spinal cord membranes was extracted in 1% octylpyranoglucoside. Protein concentrations of extracts were determined by using the BCA kit. ELISA with anti-MAG 513 confirmed the presence of MAG in both extracts (data not shown). Recombinant MAG extract (1 μg/μl total protein) in CHAPS solution and endogenous MAG extract (1 μg/μl

total protein) in octylpyranoglucoside solution were incubated with either control COS or NgR2-COS membranes (5 $\mu g/\mu l$ total protein each) at a ratio of 1:3 for 1 h on ice. Detergents in MAG extracts caused COS membranes to dissolve completely. As a control, MAG extracts were incubated with anti-MAG (mAb 513; 0.1 $\mu g/\mu l$ dialyzed against Neurobasal medium) at a ratio 1:3. Each of the three mixtures (3 μl/well) then was spotted on PDL-coated (100 μg/ml) 96-well plates (in triplicates), air dried, incubated for 15 min in 5% dialyzed FBS, and rinsed once in 1× PBS. To each well 35,000 Percoll-purified P7 CGNs were added, and plates were incubated at 37°C/5% CO_2 in a humidified incubator. After 20 h in SATO$^+$ medium the cultures were fixed and stained with TuJ1.

Quantitative analysis of neurite length. All fluorescence pictures were taken with an IX71 Olympus (Melville, NY) inverted microscope attached at the side to a DP70 digital camera. For quantification of neurite length, pictures of dissociated DRGs or CGNs with processes equal to or longer than approximately one cell body diameter were taken. Neurite length was measured from digitized images by UTHSCSA Image Tool for Windows, version 3.0. The mean and SEM of neurite-bearing cells were calculated from at least three to six independent experiments. Data were analyzed by one-way ANOVA, followed by Dunn's *post hoc* analysis or Student's *t* test with SigmaStat 3.0. All error bars that are shown indicate SEM.

Results

The Nogo receptor family members NgR1, NgR2, and NgR3 are expressed strongly in the adult brain

We identified two leucine-rich repeat (LRR) proteins in rat with a domain arrangement identical to NgR1, termed NgR2 and NgR3 (Fig. 1*A*). Toward their N-terminal end NgR1, NgR2, and NgR3 feature a characteristic and highly conserved array of eight LRRs. The LRRs are flanked N-terminally (LRRNT) and C-terminally (LRRCT) by cysteine-rich capping sequences. The LRRNT+LRR+LRRCT domains, hereafter called the LRR cluster, are connected via a less-conserved stalk sequence ("unique" domain) to a glycosylphosphatidylinositol (GPI) anchor for membrane attachment (Fig. 1*A*). The same molecules have been identified independently (Barton et al., 2003; Klinger et al., 2003; Lauren et al., 2003; Pignot et al., 2003).

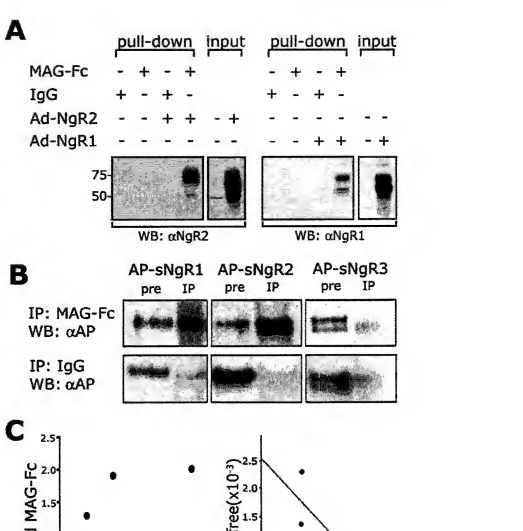

Figure 3. NgR2 binds MAG directly and with high affinity. *A*, MAG-Fc affinity precipitation of NgR1 and NgR2 from lysates of Ad-NgR1-transduced (right) or Ad-NgR2-transduced (left) COS-7 cells. Lysates of virus-infected or control (uninfected) cells were subjected to affinity precipitation with MAG-Fc or control IgG. Immunoblotting with anti-NgR1 and anti-NgR2 revealed binding of MAG to NgR2 and NgR1 (pull-down). Of note, MAG binds selectively to the high-molecular-weight forms of NgR2 and preferentially to the higher-molecular-weight forms of NgR1. The input lanes show immunoblots of total cell lysate of control, Ad-NgR1-, and Ad-NgR2-transduced cells. *B*, MAG-Fc directly binds to soluble NgR1 (AP-sNgR1) and NgR2 (AP-sNgR2), but not to NgR3 (AP-sNgR3). A control IgG does not bind to any of the soluble Nogo receptors. Input (pre) and precipitates (IP) were analyzed by immunoblotting with anti-AP. *C*, Scatchard analysis of NgR2-transfected COS-7 cells to increasing concentrations of MAG-Fc (0.1–5 nM) produced a linear plot revealing an apparent K_D of 2 nM (a representative plot of 3 independent experiments is shown on the right). The graph on the left shows the MAG-Fc saturation binding curve to NgR2-expressing COS-7 cells.

To begin to examine endogenous protein expression of NgR family members (NgRs), we raised rabbit immune sera directed against the less-conserved LRRCT and unique domain sequences of NgR1, NgR2, and NgR3. The resulting immune sera are specific as revealed by immunocytochemistry and immunoblotting of recombinant and endogenously expressed NgRs (Fig. 1*B*,*C*). In transfected COS-7 cells the myc-epitope-tagged NgR1, NgR2, and NgR3 are expressed abundantly and detected selectively by anti-NgR1, anti-NgR2, and anti-NgR3 antibodies, respectively. Endogenously expressed receptors in adult brain extracts migrate at apparent molecular weights of 65 kDa (NgR1), 65 kDa (NgR2), and as multiple bands between 35 and 90 kDa (NgR3). Multiple forms of recombinant NgR3 with a molecular weight distribution similar to the one reported here have been described previously (Pignot et al., 2003). In summary, the antisera raised against the C-terminal portion of NgR1, NgR2, and NgR3 are specific and allow selective detection of endogenously expressed NgR family members in the adult brain.

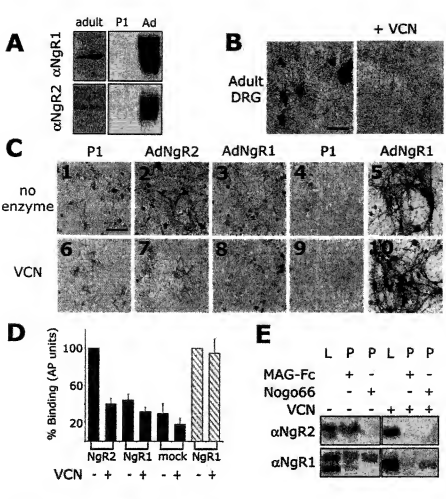

Figure 4. Ectopic expression of NgR2 in neurons is sufficient to confer sialic acid-dependent MAG binding. *A*, Immunoblotting of dissociated adult rat DRG cultures reveals expression of NgR1 and NgR2. Neonatal (P1) DRG neurons express very low levels of NgR1 and NgR2. When transduced with Ad-NgR1 or Ad-NgR2, P1 DRG neurons express high levels of NgR1 and NgR2 as revealed by Western blot analysis. *B*, Dissociated adult rat DRGs support binding of MAG-Fc in a sialic acid-dependent, VCN-sensitive manner. *C*, P1–P2 DRGs support MAG-Fc binding weakly (*C1*). After transduction with Ad-NgR2 (*C2*) or Ad-NgR1 (*C3*), the DRGs support MAG-Fc binding more strongly. Binding of MAG-Fc to control (*C6*), Ad-NgR2-transduced (*C7*), and Ad-NgR1-transduced (*C8*) DRGs is sensitive to VCN treatment. Binding of Nogo-66 to Ad-NgR1-transduced DRGs is very robust (*C9*) compared with control (uninfected) DRGs (*C4*), and Nogo-66 binding to NgR1 is not sensitive to VCN treatment (*C10*). *D*, Quantification of MAG-Fc binding to Ad-NgR2, Ad-NgR1, and mock-transduced DRGs in the absence (−) or presence (+) of VCN and binding of AP-Nogo-66 to Ad-NgR1-transfected DRGs (striped bars). MAG binding to Ad-NgR2 and AP-Nogo-66 binding to Ad-NgR1-transfected cultures is normalized to 100%. Error bars indicate SEM. *E*, MAG-Fc affinity precipitation of NgR2 and NgR1 from virally transduced DRG cultures is robust and highly sensitive to VCN treatment. Cell lysates (L) show high- and low-molecular-weight forms of NgR1 and NgR2. Western blot analysis of precipitates (P) reveals that MAG preferentially complexes with the higher-molecular-weight forms of NgR1 and NgR2. After VCN treatment NgR1 and NgR2 no longer support the binding of MAG-Fc. Moreover, VCN treatment results in a ~2–3 kDa decrease in molecular weight of NgR1 and NgR2. Binding of Nogo-66 to Ad-NgR1-transduced DRGs is not sensitive to VCN treatment. *F*, A similar VCN-dependent drop in molecular weight was observed with endogenously expressed NgR1 and NgR2 isolated from P14 rat brain. Scale bars: *B*, *C*, 100 μm.

MAG binds to NgR2 with high affinity

The structural similarities among NgR1, NgR2, and NgR3, coupled with their strong expression in the adult brain (Fig. 1*C*), prompted us to ask whether NgR2 and NgR3 support binding of any of the previously identified NgR1 ligands (Fig. 2*A*). In accordance with recent reports, AP-tagged Nogo-66 (AP-Nogo-66), chimeric MAG ectodomain (MAG-Fc), and the AP-tagged ectodomain of OMgp (OMgp-AP) avidly bind to recombinant NgR1 expressed in COS-7 cells (Fournier et al., 2001; Domeniconi et al., 2002; Liu et al., 2002; K. C. Wang et al., 2002a; Barton et al., 2003). In marked contrast, neither NgR2 nor NgR3 supports binding of AP-Nogo-66 or OMgp-AP (Fig. 2*A*). Interestingly, NgR2, but not NgR3, supports high-affinity binding of MAG-Fc, suggesting that NgR2 is a selective binding partner for MAG. To examine whether inhibitory domains of Nogo-A other than Nogo-66 interact with NgR family members, we generated AP-NiG, an amino-Nogo fragment with strong inhibitory activity (Oertle et al., 2003). No binding of AP-NiG to NgR1, NgR2, or NgR3 was observed (Fig. 2*A*). This suggests that NgRs are not receptors for amino-Nogo. Thus the Nogo receptor family members NgR1 and NgR2 are cell surface proteins with distinct, yet partially overlapping, binding preferences for myelin-derived inhibitors of axonal growth.

Because a previous study reported that NgR2 does not support MAG binding (Barton et al., 2003), we performed several control experiments to confirm the specificity of the MAG–NgR2 association. To exclude binding of the Fc portion (of MAG-Fc), rather than the MAG ectodomain to NgR2, we examined binding of an AP-Fc fusion protein. As shown in Figure 2*B*, soluble AP-Fc does not bind to NgR2. The dimerized ectodomain of Siglec 3 (Siglec 3-Fc), a MAG-related protein, does not bind to NgR2 in COS-7 cells (Fig. 2*B*). More importantly, the monoclonal anti-MAG IgG (mAb 513), previously shown specifically to block MAG-Fc binding to neurons (Collins et al., 1997), selectively blocks the NgR2–MAG interaction. A control antibody, anti-p75 IgG, does not block the NgR2–MAG association (Fig. 2*B*, *C*).

Next we asked whether NgR2 and MAG-Fc interact in solution. COS-7 cells transduced with the adenoviral vectors Ad-NgR1 or Ad-NgR2 express high levels of NgR1 and NgR2 (Fig. 3*A*). Lysates of viral vector-transduced cells then were subjected to affinity precipitation with MAG-Fc or control IgG. Consistent with our binding studies in COS-7 cells, MAG-Fc binds more avidly to NgR2 than to NgR1. A control IgG forms a complex with neither NgR1 nor NgR2 (Fig. 3*A*). Of note, MAG binds preferentially to higher (presumably fully glycosylated) molecular weight forms of NgR2. A similar but less-pronounced binding preference was observed toward the larger forms of NgR1 (Fig. 3*A*). Next, to examine

whether MAG-Fc binds NgR1 and NgR2 directly, we performed affinity precipitation experiments with MAG-Fc and soluble AP-tagged Nogo receptors (AP-sNgR1, AP-sNgR2, and AP-sNgR3) isolated from serum-free supernatants of transiently transfected HEK293T cells. AP-sNgR1 and AP-sNgR2, but not AP-sNgR3, form a complex with MAG-Fc (Fig. 3*B*). This indicates that the ectodomain of MAG interacts with NgR1 and NgR2 directly.

In a semi-quantitative experiment we compared the binding of serially diluted MAG with NgR1 and NgR2 expressed in COS-7 cells (supplemental Fig. 1, available at www.jneurosci.org as supplemental material). The experiment confirmed that MAG binds with higher affinity, approximately four to eight times stronger, to NgR2 than to NgR1. In COS-7 cells the coexpression of NgR1 and NgR2 does not enhance MAG binding when compared with NgR2 alone (data not shown). To measure directly the affinity of the MAG–NgR2 association, we performed a Scatchard plot analysis of MAG-Fc binding to NgR2-expressing COS-7 cells (Fig. 3*C*). Plotting of the saturation binding data revealed an apparent K_D of 2 nM. Previously determined affinity constants for the NgR1–MAG interaction are 8 and 20 nM (Domeniconi et al., 2002; Liu et al., 2002). Together, our studies reveal that MAG exhibits the following binding preferences for NgR family members: NgR2 > NgR1 ≫ NgR3.

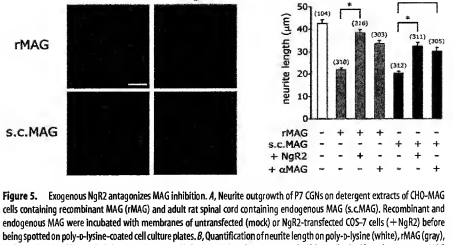

Figure 5. Exogenous NgR2 antagonizes MAG inhibition. *A*, Neurite outgrowth of P7 CGNs on detergent extracts of CHO-MAG cells containing recombinant MAG (rMAG) and adult rat spinal cord containing endogenous MAG (s.c.MAG). Recombinant and endogenous MAG were incubated with membranes of untransfected (mock) or NgR2-transfected COS-7 cells (+NgR2) before being spotted on poly-D-lysine-coated cell culture plates. *B*, Quantification of neurite length on poly-D-lysine (white), rMAG (gray), and s.c.MAG (black) revealed that membranes of NgR2-expressing, but not control, COS-7 cells significantly attenuate MAG inhibition. A similar effect was achieved when MAG extracts were preincubated with anti-MAG (mAb 513), a function-blocking MAG antibody. The number of neurites quantified for each condition is indicated in parentheses. Results are presented as the mean ± SEM from three independent experiments. *$p < 0.05$, significantly different from CGNs grown on rMAG and s.c.MAG; Kruskal–Wallis one-way ANOVA (*post hoc* Dunn's test). Scale bar, 40 μm.

Ectopic expression of NgR2 in neonate neurons is sufficient to confer sialic acid-dependent binding of MAG

Neonatal DRG neurons express very low levels of NgR1 and NgR2 and support MAG binding poorly when compared with adult DRGs (Fig. 4). Consistent with this observation, immunoblotting of cultured DRG neurons revealed stronger expression of NgR1 and NgR2 in adulthood (Fig. 4*A*). To examine whether ectopic expression of NgR1 or NgR2 in P1–P2 DRG neurons is sufficient to confer MAG binding, we transduced cultures with Ad-NgR1 and Ad-NgR2. Virally transfected neurons express high levels of NgR1 and NgR2 (Fig. 4*A*). Consistent with studies in COS-7 cells, Ad-NgR1- and Ad-NgR2-transduced DRG neurons support the binding of MAG-Fc. Moreover, MAG shows preferential binding to NgR2 (Fig. 4*C*,*D*). To assess whether neuronally expressed NgR1 and NgR2 support MAG binding in a sialic acid-dependent manner, we treated virally transduced cultures with VCN. Quantification of MAG binding to DRG neurons after VCN treatment revealed a 60 and 31% decrease to Ad-NgR2- and Ad-NgR1-transduced cultures, respectively (Fig. 4*C*,*D*). Consistent with pervious studies (DeBellard et al., 1996), MAG binding to uninfected DRG cultures is also VCN-sensitive (Fig. 4*D*). Binding of Nogo-66 to Ad-NgR1-transduced DRG cultures, however, is not sensitive to VCN treatment (Fig. 4*C*,*D*). To address directly whether MAG binds to NgR1 and NgR2 in a sialic acid-dependent manner, we performed affinity precipitation experiments from DRG lysates using MAG-Fc. As shown in Figure 4*E*, MAG-Fc forms a complex with NgR2 and, to a lesser extent, with NgR1 in lysates of virally transduced DRGs. MAG-Fc preferentially interacts with the higher-molecular-weight forms of neuronally expressed NgR1 and NgR2 (Fig. 4*E*). In stark contrast, when pretreated with VCN, NgR1 and NgR2 no longer complex with MAG-Fc. NgR1 maintains Nogo-66 binding in VCN-treated cultures (Fig. 4*E*). Moreover, we observed a ~2–3 kDa drop in the molecular weight of NgR1 and NgR2 in virally transduced DRG cultures treated with VCN (Fig. 4*E*). Importantly, a similar VCN-dependent shift in molecular weight was observed for endogenous NgR1 and NgR2 isolated from 2-week-old rat brain (Fig. 4*F*). Together, these experiments indicate that ectopic expression of NgR1 and NgR2 in primary neurons is sufficient to confer MAG binding. MAG binds to NgR1 and NgR2 in a sialic acid-dependent and VCN-sensitive manner. Loss of MAG binding appears to coincide with asmall but significant drop in molecular weight of NgR1 and NgR2.

Exogenous NgR2 has MAG/myelin antagonistic capacity

Given the strong affinity of NgR2 for MAG, we next examined whether exogenously added NgR2 has MAG/myelin antagonistic function. To inhibit neurite outgrowth, we plated P7 CGNs on substrata adsorbed with a detergent extract of either CHO-MAG cell membranes or adult rat spinal cord membranes that contain MAG (Vyas et al., 2002). On recombinant MAG (rMAG from

→

Figure 6. Ectopic NgR2 in neonatal DRGs confers MAG inhibition. *A*, Neonatal DRGs transduced with Ad-NgR2 abundantly express NgR2. Ectopic NgR2 is localized to neurites and growth cones, as revealed by anti-NgR2 and Tuj1 double immunofluorescence. *B*, DRGs transduced with Ad-NgR1 or Ad-NgR2 were seeded on confluent monolayers of CHO (control) or CHO-MAG cells. Neurons expressing ectopic NgR1 or NgR2 were identified by double immunofluorescence labeling with anti-NgR1 or anti-NgR2 and Tuj1. *C*, Quantification of neurite length. Neurites of untransduced or Ad-RFP-transduced DRGs on CHO-MAG are 15 and 20% longer than on CHO feeder layers, respectively. DRGs infected with Ad-NgR1 or Ad-NgR2 before plating on CHO-MAG show a 22 and 32% decrease in neurite length, respectively. The number of neurites measured for each condition is indicated in parentheses. Results are presented as the mean ± SEM from three independent experiments. *$p < 0.05$, significantly different from Ad-RFP-transduced DRGs; Kruskal–Wallis one-way ANOVA (*post hoc* Dunn's test). On CHO control cells Ad-NgR2-transduced DRGs show a small but statistically nonsignificant decrease in neurite length. Scale bar: (in *B*), 50 μm.

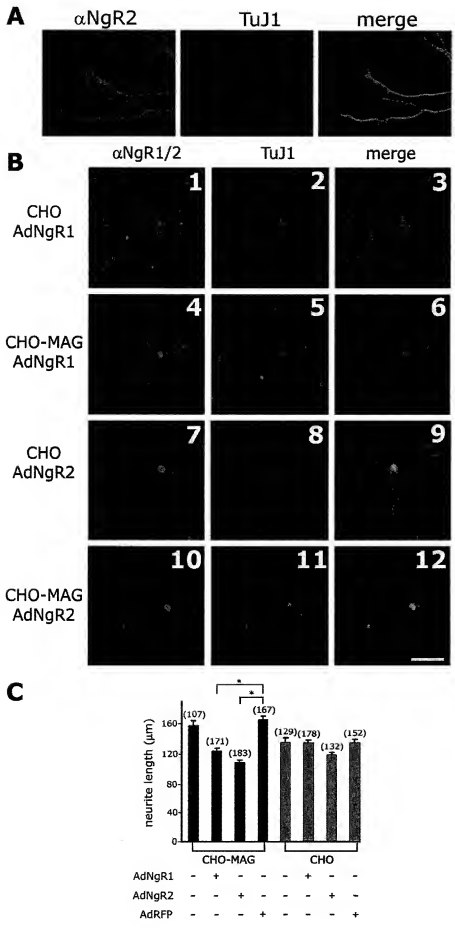

CHO-MAG cells) and endogenous MAG (s.c.MAG from spinal cord) substrate, neurite length decreases to 51% (rMAG) and 47% (s.c.MAG) of CGNs grown on control substrate (Fig. 5). To show directly that inhibition is attributable to the presence of MAG, we preincubated inhibitory extracts with anti-MAG (mAb 513), a function-blocking antibody. Anti-MAG greatly attenuated the inhibition of CGNs on both substrates. Neurite length increases to 81% (rMAG) and 70% (s.c.MAG) of controls (Fig. 5*B*). More importantly, preincubation of MAG extracts with NgR2-COS-7 membranes (+NgR2) greatly attenuated inhibition of CGNs compared with MAG extracts incubated with control COS-7 membranes (mock). In the presence of exogenous NgR2 the neurite length increased to 89% (rMAG) and 74% (s.c. MAG) of controls (Fig. 5*A*,*B*). To rule out the possibility that exogenous NgR2 attenuates MAG inhibition indirectly via binding to NgR1, we asked whether NgR1 interacts with NgR2. As shown in supplemental Figure 2 (available at www.jneurosci.org as supplemental material), affinity precipitation with NgR1-Fc from lysates of Ad-NgR2-transduced COS cells did not reveal an NgR1–NgR2 association. As a positive control we show that NgR1-Fc binds strongly to AP-Nogo-66, but not to AP-NiG. Thus soluble NgR1 and NgR2 do not appear to interact with each other. Taken together, our experiments suggest that binding of soluble NgR2 masks the growth inhibitory domain or domains of MAG and that exogenous NgR2 has MAG/myelin antagonistic capacity *in vitro*.

Ectopic expression of NgR2 in neonate DRG neurons is sufficient to confer MAG inhibition

MAG is a bifunctional guidance molecule; it promotes growth of young neurons and inhibits growth at more mature stages. Consistent with previous reports, we observed that MAG promotes neurite growth of neonatal DRG neurons (Johnson et al., 1989). When cultured on monolayers of CHO-MAG or CHO cells, neurites of P1–P2 DRGs grow 15–20% longer on CHO-MAG than on CHO substrate (Fig. 6). To ask whether ectopic NgR1 or NgR2 is sufficient to confer MAG inhibition on NGF-responsive DRG neurons, we transduced dissociated DRGs for 3 h with Ad-NgR1 or Ad-NgR2 before plating them on CHO-MAG or CHO feeder layers. After 20 h the cultures were fixed and stained by double immunofluorescence for neuron-

specific class III β-tubulin (TuJ1) and NgR1 or NgR2. Ectopic NgR2 and NgR1 (data not shown) are localized to cell bodies, neurites, and growth cones of transduced neurons (Fig. 6A). Quantification of neurite lengths on CHO-MAG cells revealed a decline in fiber length of 22% for NgR1$^+$ and 32% for NgR2$^+$ neurons when compared with Ad-RFP-transduced neurons. On CHO feeder cells the NgR2$^+$ DRGs show a small decrease in fiber length that is not statistically significant from Ad-RFP- or Ad-NgR1-transduced DRGs (Fig. 6B,C). Together, these experiments show that, on MAG substrate, ectopic NgR1 and NgR2 lead to a significant decrease in fiber length. Thus, similar to NgR1, NgR2 functions as an inhibitory receptor for MAG.

Ectopic expression of NgR2 in postnatal CGNs augments the MAG inhibitory response

In a parallel experiment to examine whether NgR2 participates in MAG inhibitory responses, we used P7 CGNs. P7 CGNs strongly express NgR1 and p75, but not NgR2 (Fig. 7B). On CHO-MAG feeder layers the neurite growth of P7 CGNs is reduced significantly compared with CGNs grown on CHO feeder layers. Because NgR2 binds MAG more strongly than NgR1, we ectopically expressed NgR2 in P7 CGN to examine whether NgR2 functions as a productive receptor that increases MAG inhibition or behaves as a dominant-negative receptor that binds MAG unproductively. In the latter case, ectopic NgR2 may sequester MAG away from NgR1 and thus lead to an increase in neurite length. Purified P7 CGNs were transfected by nucleofection (Maasho et al., 2004) and cultured on control CHO or CHO-MAG feeder layers (Fig. 7A). Neuronal transfection efficiencies of >40% were achieved, as revealed by double immunofluorescence with anti-GFP and the neuron-specific antibody TuJ1. Transfected GFP$^+$ neurons cultured on CHO cells grow long neurites within 24 h (Fig. 7A,C). When plated on CHO-MAG monolayers, neurite outgrowth of GFP$^+$ CGNs is strongly inhibited. Quantification of neurite length of GFP$^+$ CGNs on CHO-MAG cells revealed a significant (53%) decrease in length compared with controls on CHO cells (Fig. 7D). When cotransfected with *NgR2* and *GFP* plasmid DNA (ratio, 3:1), GFP$^+$ neurons coexpress NgR2, as shown by anti-NgR2 immunocytochemistry and immunoblotting of transfected CGNs lysates (Fig. 7C), and hereafter are referred to as NgR2$^+$ CGNs. On CHO cells the neurite length of NgR2$^+$ (34 ± 3 μm) and GFP$^+$ CGNs (36 ± 3 μm) is very similar. On CHO-MAG cells, how-

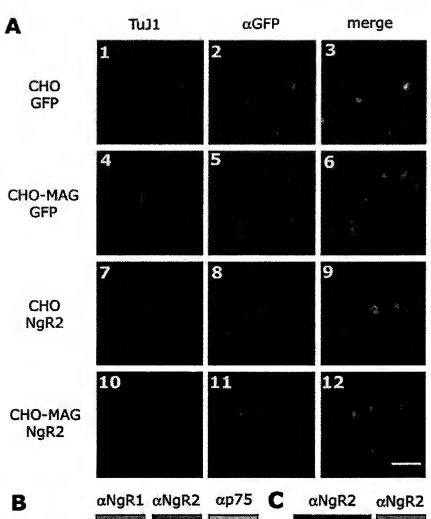

Figure 7. Ectopic expression of NgR2 in P7 CGNs augments MAG inhibition. *A*, P7 rat CGNs were purified in a discontinuous Percoll gradient and transfected by nucleofection with expression plasmids for EGFP (*A1–A6*) and a plasmid mixture for EGFP and NgR2 (*A7–A12*). After transfection, the neurons were seeded on confluent monolayers of CHO (control) or CHO-MAG cells. Transfected neurons were identified by double immunofluorescence labeling with anti-GFP (green) and TuJ1 (red). *B*, Immunoblotting of untransfected P7 CGN lysates revealed expression of NgR1 and p75, but not NgR2. *C*, After nucleofection, the CGNs express NgR2, as shown by anti-NgR2 ICC (left) and Western blot analysis (right). *D*, Quantification of neurite length. The number of neurites measured for each condition is indicated in parentheses. Results are presented as the mean ± SEM from four independent experiments. *$p < 0.008$, significantly different from GFP$^+$ CGNs on CHO-MAG cells. Fiber length of GFP$^+$ and NgR2$^+$ CGNs on CHO is not significantly different; Kruskal–Wallis one-way ANOVA (*post hoc* Dunn's test). Scale bar, 30 μm.

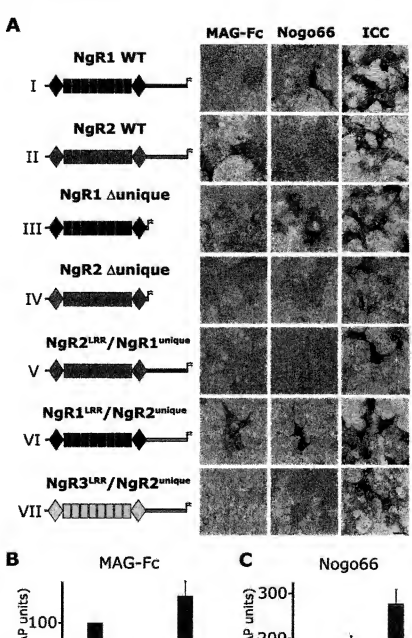

Figure 8. Structural basis of the NgR2–MAG association. *A*, A chimeric receptor strategy was pursued to identify the NgR2 domains necessary for MAG binding. Wild-type and mutant receptors were expressed transiently in COS-7 cells, and surface expression and distribution were confirmed by anti-NgR1 or anti-NgR2 ICC under nonpermeabilizing conditions. Binding of MAG-Fc was detected with an anti-human Fc AP-conjugated antibody and compared with AP-Nogo-66. Wild-type NgR1 and NgR1-Δunique support the binding of Nogo-66 and MAG. In stark contrast, wild-type NgR2, but not NgR2-Δunique, supports high-affinity MAG binding. Thus, the NgR2-unique domain is necessary for high-affinity MAG binding. Chimera VII indicates that the NgR2-unique domain is not sufficient for MAG binding. Of note, chimera VI, composed of the NgR1–LRR cluster fused to the NgR2-unique domain, supports high-affinity binding of Nogo-66 and MAG-Fc. *B*, Quantification of MAG-Fc (17 nM) binding to wild-type and mutant receptors in relative AP units normalized to wild-type NgR2 (100%). Chimera VI supports MAG binding with greater affinity than wild-type NgR2. *C*, Quantification of AP-Nogo-66 (10 nM) binding to wild-type and mutant receptors in relative AP units normalized to wild-type NgR1 (100%). Constructs III and VI support AP-Nogo-66 binding with greater affinity than wild-type NgR1. Results are presented as the mean ± SEM from three to five independent binding experiments, normalized to receptor cell surface expression. Scale bar, 10 μm.

ever, NgR2^{+} CGNs show a significant decrease (41%) in neurite length when compared with GFP^{+} CGNs (Fig. 7*D*). In summary, these experiments reveal that ectopic expression of NgR2 in CGN, a cell type that normally does not express NgR2, is sufficient to increase the MAG inhibitory response greatly. Thus we conclude that ectopic NgR2 in CGNs does not behave as a dominant-negative MAG receptor but, rather, functions as a productive receptor that mediates MAG inhibition.

Structural basis of the NgR2–MAG association

Previous studies have shown that the NgR1–LRR cluster (NgR1Ecto$^{1-310}$) is necessary and sufficient for the binding of Nogo-66, MAG, and OMgp (Fournier et al., 2002; K. C. Wang et al., 2002a; X. Wang et al., 2002; Barton et al., 2003). Given the high degree of conservation between NgR1 and NgR2 over the extent of the LRR cluster, we first asked whether the corresponding sequences of NgR2, including the LRRNT-LRR-LRRCT domains (NgR2Ecto$^{1-313}$), are sufficient to support high-affinity MAG binding. Consistent with pervious reports, deletion of the NgR1-unique domain (NgR1$^{\Delta unique}$) does not alter the binding properties of NgR1 toward Nogo-66, OMgp (data not shown), or MAG-Fc. Significantly, an analogous construct of NgR2 lacking the unique domain (NgR2$^{\Delta unique}$) supports MAG-Fc binding very poorly compared with full-length NgR2 (Fig. 8). This indicates that the NgR2Ecto$^{1-313}$ is not sufficient for high-affinity MAG binding and that sequences in the NgR2-unique domain are important for MAG binding.

To examine whether the NgR2-unique domain is sufficient to support MAG binding, we fused the NgR3–LRR cluster to the NgR2-unique domain, resulting in chimera NgR3^{LRR}/NgR2^{unique}. Similar to wild-type NgR3 (Fig. 2*A*), NgR3^{LRR}/NgR2^{unique} does not support MAG-Fc or Nogo-66 binding (Fig. 8*A*,*B*). Together, this suggests that the NgR2-unique domain is necessary but not sufficient for high-affinity MAG binding. Next we asked whether the NgR1-unique domain, when fused to the NgR2–LRR cluster, restores high-affinity MAG binding and, conversely, whether the NgR2-unique domain enhances binding to the NgR1–LRR cluster. We generated two chimeric receptors, NgR2^{LRR}/NgR1^{unique} and NgR1^{LRR}/NgR2^{unique}, in which the unique domains of NgR1 and NgR2 were swapped (Fig. 8*A*). Interestingly, swapping of the NgR1- and NgR2-unique domains reverses the MAG binding preferences; similar to wild-type NgR2, NgR1^{LRR}/NgR2^{unique} binds MAG

with high affinity, and, vice versa, $NgR2^{LRR}/NgR1^{unique}$ binds MAG with lower affinity similar to wild-type NgR1 (Fig. 8*B*). Of note, chimera $NgR1^{LRR}/NgR2^{unique}$ also binds strongly to Nogo-66 (Fig. 8*B*) and OMgp (data not shown). Thus chimera $NgR1^{LRR}/NgR2^{unique}$ embodies the high-affinity binding capacity of NgR2 toward MAG and that of NgR1 toward Nogo-66 and OMgp. The complementary construct, chimera $NgR2^{LRR}/NgR1^{unique}$, binds MAG weakly and does not support binding of Nogo-66 (Fig. 8*B*) or OMgp (data not shown). Immunocytochemistry of transfected COS-7 under nonpermeabilizing conditions was used to confirm surface expression of all receptor constructs (Fig. 8*A*).

The relative binding affinity (in AP units) of MAG-Fc for each receptor construct was assessed quantitatively and normalized to cell surface receptor expression. The average binding affinities of MAG-Fc and AP-Nogo-66 to receptor chimera, normalized to the wild-type NgR2–MAG (= 100%) and wild-type NgR1–Nogo-66 (= 100%) interaction, are shown in Figure 8, *B* and *C*. Of note, chimera $NgR1^{LRR}/NgR2^{unique}$ supports AP-Nogo-66 binding 2.7-fold stronger than wild-type NgR1. In addition, $NgR1^{LRR}/NgR2^{unique}$ supports MAG binding with fivefold and 1.2-fold greater affinity than wild-type NgR1 and NgR2, respectively. In summary, our structural analysis of the NgR2–MAG association suggests that the NgR2–LRR cluster and the NgR2-unique domain work cooperatively and are both necessary for high-affinity MAG binding. Whereas the NgR2–LRR cluster is necessary and sufficient to support MAG binding weakly, the NgR2-unique domain is necessary but not sufficient for high-affinity MAG binding. This is in sharp contrast to the NgR1-unique domain, which is not necessary for maximal binding of MAG or Nogo-66 to NgR1. Thus the structural basis of MAG binding appears to be distinct and only partially conserved between NgR1 and NgR2. Although the NgR1 ligand-binding domain (LBD) is composed of the LRR cluster only, the NgR2 LBD is more extended, including the LRR cluster as well as sequences in the juxtaposed unique (stalk) domain.

NgR2 is an axon-associated glycoprotein abundantly expressed in the adult brain

Based on our functional studies in primary neurons, the selectivity, and sialic acid dependence of the MAG–NgR2 association, we hypothesized that NgR2 is a novel MAG receptor. If NgR2 is indeed a MAG receptor, protein expression is expected to be associated with projection neurons and to include axons of myelinated fiber tracts. To begin to address the tissue distribution of NgR2 and its relation and relative abundance to NgR1, we used a combination of *in situ* hybridization, immunohistochemistry, and tissue immunoblotting. *In situ* hybridization with RNA probes directed against the coding region of the less-conserved unique portions of *NgR1* and *NgR2* revealed that both transcripts are expressed broadly in the mature CNS and localized primarily to cell bodies of projection neurons. In the retina, for example, *NgR2* is expressed in the ganglion cell layer (GCL) and the inner segment of the inner granule cell layer (IGL), but not in the outer granule cell layer (OGL). A very similar staining pattern, but with lower intensity, was found for *NgR1* (Fig. 9*A*). To examine whether NgR1 and NgR2 are localized to axons, we performed immunohistochemistry on adult retina. In line with our *in situ* hybridization data and consistent with a role in axon–glia interaction, anti-NgR1 and anti-NgR2 IgG decorate retinal cell soma in the GCL and axons of the optic fiber layer (OFL). In addition, cell bodies in the IGL are labeled with anti-NgR2 and to a lesser extent with anti-NgR1 (Fig. 9*A*). In cross sections of adult spinal cord *NgR2* expression is restricted to gray matter and is absent from white matter. Particularly robust labeling is confined to presumptive motor neurons in the ventral horn. Many large- and small-caliber sensory neurons in DRGs express *NgR2*; the expression appears broad but heterogeneous, with some neurons being labeled more intensely (Fig. 9*B*). To study the relative abundance of NgR1 and NgR2 in different brain regions, we dissected specific areas and subjected them to immunoblotting, using our anti-NgR1- and anti-NgR2-specific immune sera (Fig. 9*C*). Consistent with histochemical studies (Fig. 9*A*,*B*) (Pignot et al., 2003), both receptors are expressed broadly in the CNS, including retina, olfactory bulb, septum, neocortex, entorhinal cortex, hippocampus, striatum, and thalamus (Fig. 9*C*). Although expression of NgR1 and NgR2 appears to be very broad, we also noticed clear differences in the relative abundance of NgR1 and NgR2 within specific brain regions. In the retina, for example, NgR2 is much more prominent than NgR1; conversely, in the thalamus NgR1 is more prominent than NgR2. Robust expression of NgR1 and NgR2 is found in the neocortex, entorhinal cortex, hippocampus, and striatum (Fig. 9*C*). Much weaker expression of NgR1 and NgR2 is observed in the olfactory bulb and the septum. Taken together, the tissue distribution patterns of NgR1 and NgR2 are overlapping, yet distinct, including numerous populations of projection neurons. Moreover, NgR2, similar to NgR1 (X. Wang et al., 2002), is found on myelinated axons. Given that MAG is localized to myelin sheets immediately adjacent to the axon (Trapp et al., 1989), NgR1 and NgR2 are well positioned to function as neuronal MAG receptors *in vivo*.

Neural NgR2 is localized to lipid rafts

Recent studies have shown that a number of neuronal receptors that regulate axon growth and guidance are associated with cholesterol- and sphingolipid-enriched membrane microdomains called lipid rafts (Tsui-Pierchala et al., 2002; Guirland et al., 2004). Specifically, several MAG receptor components, including NgR1, p75, and GT1b, are localized to lipid rafts (Vinson et al., 2003). Because MAG in myelinating glia also is associated with lipid rafts, a model has been proposed in which MAG function involves lipid raft-to-lipid raft interaction on opposing cell membranes. To begin to address whether NgR2 may participate in such interactions, we isolated Triton X-100-insoluble caveolin-positive membrane fractions from P14 rat brain. Immunoblotting with anti-NgR1 and anti-NgR2 revealed that both receptors are found nearly exclusively within lipid rafts (Fig. 9*D*). Thus NgR2 may be part of a bidirectional signaling system that regulates MAG inhibition of neurite outgrowth and maintenance of myelin integrity.

Discussion

Here we report on the identification of NgR2 as a neuronal MAG receptor that functions in neurite growth inhibition. NgR2 supports high-affinity and sialic acid-dependent binding of MAG. Consistent with a role as MAG receptor, NgR2 is expressed in postnatal and adult neurons and localized to axons of myelinated fiber tracts. Ectopic expression of NgR2 in neonatal DRG neurons is sufficient to inhibit growth on MAG substrate. In more mature neurons the ectopic expression of NgR2 augments the MAG inhibitory response, indicating that NgR2 is a functional MAG receptor. Soluble NgR2 has MAG antagonistic function and promotes neurite growth on myelin substrate *in vitro*. Finally, molecular studies of the NgR2–MAG association revealed that the LRR cluster and unique domain of NgR2 are necessary for high-affinity MAG binding. Taken together, our results sug-

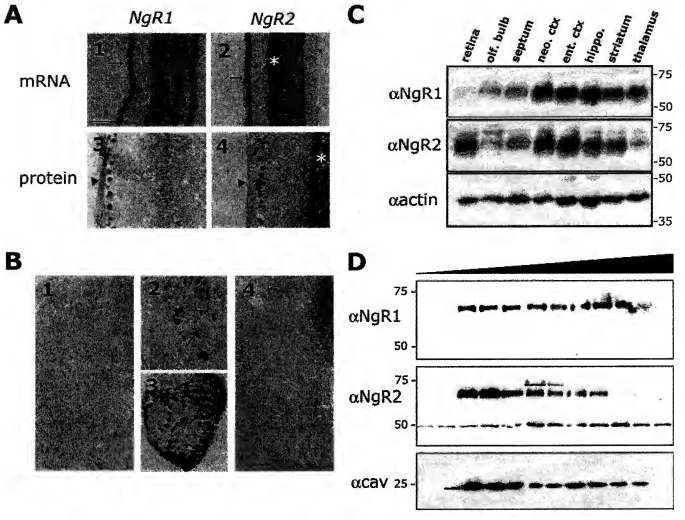

Figure 9. NgR2 is an axon-associated receptor broadly expressed in the postnatal and adult CNS. *A*, Comparison of NgR1 and NgR2 expression in adult retina of the rat. *In situ* hybridization shows expression of *NgR1* (*A1*) in presumptive retinal ganglion cells (RGCs; arrow) and the inner part of the IGL; see asterisk. A very similar but more robust expression in the retina was observed for *NgR2* (*A2*). Consistent with the mRNA distribution, anti-NgR1 and anti-NgR2 label the cell bodies of RGCs and axons in the optic fiber layer (arrowhead). Anti-NgR1 labels the IGL weakly, and anti-NgR2 labels the IGL strongly (asterisk). *B*, Cross section of adult spinal cord at mid-thoracic level; dorsal is to the top (*B1*, *B2*, *B4*). *NgR2* is expressed broadly in spinal gray matter but is absent from white matter (*B1*, *B2*). Strong labeling is associated with presumptive motor neurons in the ventral horn (*B2*, arrow). Many small- and large-caliber sensory neurons in adult DRGs express *NgR2* (*B3*). Strongly labeled DRG cells (arrow) are interspersed with weakly labeled cells (*B3*). No signal was detected with a DIG-labeled sense RNA probe (*B4*). *C*, Anti-NgR1 and anti-NgR2 immunoblot of different brain regions revealed broad expression of NgR1 and NgR2 in the mature CNS. The same blot was probed serially with anti-NgR2, anti-NgR1, and anti-actin (as a loading control); see Results for details. *D*, In brain, the NgR1 and NgR2 are localized to lipid rafts. Triton X-100-insoluble lipid rafts were isolated from P14 brain extracts by flotation in a sucrose gradient and were subjected to immunoblotting with anti-NgR1, anti-NgR2, and anti-caveolin. Scale bars: *A1*, *A2*, 200 μm; *A3*, *A4*, *B2*, *B3*, 100 μm; *B1*, *B4*, 250 μm.

gest that NgR2, together with NgR1, coordinates MAG/myelin inhibitory neuronal responses.

NgR2 supports MAG binding in a sialic acid-dependent manner

MAG is a sialic acid-binding lectin, and multiple lines of evidence show that MAG inhibits growth in a sialic acid-dependent manner (DeBellard et al., 1996; Shen et al., 1998; Vinson et al., 2001; Vyas et al., 2002). Sialic acid binding alone, however, is not sufficient to bring about MAG inhibition (Tang et al., 1997). This suggests that in a functional recognition complex MAG is engaged in multiple interactions, at least one of which is sialic acid-dependent. Complex gangliosides have been identified as sialic acid-dependent MAG ligands that function in growth inhibition (Yang et al., 1996; Collins et al., 1997; Vinson et al., 2001; Vyas et al., 2002). In addition, binding of MAG-Fc to primary neurons and neuroblastoma cells is trypsin- and VCN-sensitive (DeBellard et al., 1996; DeBellard and Filbin, 1999; Strenge et al., 1999), arguing for the existence of a cell surface protein or proteins that support high-affinity MAG binding. Consistent with this idea, affinity precipitation with immobilized MAG-Fc identified specific protein interactions, some of which are sialic acid-dependent (DeBellard and Filbin, 1999; Strenge et al., 1999). Whether this is a reflection of MAG binding to a neuronal sialoglycoprotein or sialoglycoproteins or protein–ganglioside complexes, however, remains unknown. Although several MAG binding proteins have been characterized (Franzen et al., 2001; Strenge et al., 2001), NgR1 is the first binding protein directly shown to be part of a functional MAG receptor complex, yet the observation that MAG binding to NgR1 is VCN-insensitive and not modulated by the presence of GT1b adds an unexpected twist to the characterization of the neuronal MAG receptor (Domeniconi et al., 2002; Liu et al., 2002).

Because many binding studies probing the lectin activity of MAG were performed on primary neurons, we adopted a neuronal culture system to examine whether NgR1 and/or NgR2 sup-

ports MAG binding in a sialic acid-dependent manner. We found that in neonatal DRGs the ectopic expression of NgR2 (and to a lesser extent NgR1) is sufficient to confer high-affinity and sialic acid-dependent MAG binding. Affinity precipitation studies with MAG-Fc, similar to the ones originally used to probe binding partners on neuronal cells (DeBellard and Filbin, 1999; Strenge et al., 1999), showed that MAG binding to NgR1 and NgR2 is VCN-sensitive. This contrasts with studies in non-neuronal cells in which NgR1 (Domeniconi et al., 2002; Liu et al., 2002) and NgR2 (K. Venkatesh and R. Giger, unpublished data) support MAG binding in a sialic acid-independent manner. Because NgR1 and NgR2 normally are expressed in neurons, we propose that in a neuronal environment NgR1 and NgR2 are part of a high-affinity and sialic acid-dependent MAG recognition complex. Thus our data fit a model in which NgR1 and NgR2 harbor sialic acid-dependent as well as sialic acid-independent MAG docking sites. For maximal binding strength both sites are necessary. An important next question concerns the elucidation of the molecular basis of the sialic acid dependence of the MAG–NgR2 and MAG–NgR1 interactions in neurons.

We observed that VCN treatment of neuronally expressed NgR1 and NgR2 causes a small but significant drop (~2–3 kDa) in the molecular weight of both receptors. This indicates that both receptors either are highly sialylated glycoproteins (~10 terminal sialic acid residues) or alternatively associate with gangliosides in a VCN-sensitive but SDS-resistant manner. Given that NgR1 occurs as multiple isoelectric variants with a pI range of 6–8 (our unpublished observation), a large number of terminal sialic acids appear to be unlikely. SDS-resistant interactions of proteins with gangliosides, on the other hand, have been reported, most notably p75 binding to GT1b (Yamashita et al., 2002). Interestingly, the molecular weight of GT1b and other MAG-binding gangliosides is ~2 kDa. Because gangliosides support MAG binding in a sialic acid-dependent manner and are necessary for MAG inhibition (Vyas et al., 2002), it is tempting to speculate that in neurons NgR1 and NgR2 associate with a specific ganglioside or gangliosides to form a high-affinity MAG-binding complex.

NgR2 is a neuronal MAG receptor that mediates growth inhibition

To examine whether NgR2 functions as a neuronal MAG receptor, we expressed NgR2 in neonatal DRGs and P7 CGNs, two cell types that normally do not express NgR2. Ectopic expression of NgR1 or NgR2 in NGF-responsive DRG neurons results in a significant decrease in neurite length on CHO-MAG, but not on control CHO feeder cells. This suggests that ectopic NgR2, similar to NgR1, functions as a neuronal MAG receptor that mediates growth inhibition. Ectopic NgR1 and NgR2 abolish the growth-promoting effect of MAG on neonatal DRG neurons, resulting in fiber length that is comparable to that observed on control CHO feeder layers. The relatively modest decrease in fiber length observed in $NgR1^+$ and $NgR2^+$ DRG neurons is somewhat surprising, given the strong inhibitory activity of MAG toward more mature neurons. In light of the fact that neonatal DRG neurons are still neurotrophin-dependent, it is likely that they are in a "primed" state, and thus forced expression of NgR1 or NgR2 may not lead to a robust MAG inhibitory response (Cai et al., 1999). Alternatively, MAG inhibition may be limited because a receptor component or components other than NgR1 or NgR2 are not expressed sufficiently in neonatal DRG. Given that MAG-signaling components are present in embryonic neurons of different origin (Liu et al., 2002; Wong et al., 2002), this, however, appears to be unlikely. Although our studies in DRGs show that ectopic NgR1 and NgR2 lead to a decrease in neurite growth on CHO-MAG cells, we formally cannot distinguish between the following two possibilities: (1) NgR1 and NgR2 are functional MAG receptors that mediate inhibition, and (2) ectopic NgR1 and NgR2 bind MAG unproductively, sequestering it away from a receptor system that normally promotes growth of neonatal DRG neurons; as a result, neurite length is decreased.

Our interpretation that ectopic NgR2 mediates MAG inhibition in neonatal DRG neurons is consistent with the NgR2 gain-of-function studies in postnatal CGNs. Forced expression of NgR2 in CGNs greatly increases the MAG inhibitory response. Together, these findings indicate that NgR2 does not function as a decoy receptor that binds MAG unproductively but, rather, operates as a high-affinity MAG receptor that brings about inhibition.

Structural insights in ligand–receptor interactions

While this manuscript was in preparation, a study reported that NgR2 does not support MAG binding, a finding conflicting with our observations (Barton et al., 2003). The main difference between the two studies is that Barton et al. (2003), used soluble AP-MAG, whereas we used MAG-Fc, a bioactive form of MAG, for receptor binding. To compare the two ligands directly, we generated AP-MAG. Consistent with Barton et al. (2003), NgR1, but not NgR2, selectively supports binding of AP-MAG (supplemental Fig. 1, available at www.jneurosci.org as supplemental material). When coupled with our finding that the structural basis of MAG binding is different for NgR1 and NgR2, we propose that AP tagging of MAG sterically interferes with binding to NgR2, but not to NgR1.

NgR2 and MAG signaling

Similar to NgR1, NgR2 is linked to the outer leaflet of the neuronal plasma membrane by a GPI anchor. Thus NgR2-mediated MAG inhibition depends on the interaction with additional receptor components, at least one of which is expected to possess a cytoplasmic domain. Obvious signal-transducing candidates for NgR2 are the pan-neurotrophin receptor p75 (K. C. Wang et al., 2002b; Wong et al., 2002) and Lingo-1 (Mi et al., 2004). Alternatively, binding of NgR2 to NgR1 in *cis* may lead to an indirect activation of p75/Lingo-1. Our preliminary studies indicate that NgR2 does not associate with p75 in neurons (Chivatakarn et al., 2004), raising the interesting possibility that p75-independent mechanisms exist to bring about MAG inhibition.

Although MAG has received most attention for its role as an inhibitor of axonal regeneration, in steady state the MAG function has been attributed to stabilization of myelin–axon interactions by binding to complementary ligands on the axolemma (Schachner and Bartsch, 2000). Growing evidence suggests that MAG is a bifunctional molecule that, with binding to neuronal cell surface ligands, signals to oligodendrocytes (Umemori et al., 1994; Sun et al., 2004). It will be interesting to explore whether NgR1 and NgR2, in addition to their function as MAG/myelin receptors, serve as neuronal MAG ligands that contribute to the stability of myelin sheets and their associated axons *in vivo*.

References

Barton WA, Liu BP, Tzvetkova D, Jeffrey PD, Fournier AE, Sah D, Cate R, Strittmatter SM, Nikolov DB (2003) Structure and axon outgrowth inhibitor binding of the Nogo-66 receptor and related proteins. EMBO J 22:3291–3302.

Bartsch U, Bandtlow CE, Schnell L, Bartsch S, Spillmann AA, Rubin BP, Hillenbrand R, Montag D, Schwab ME, Schachner M (1995) Lack of

evidence that myelin-associated glycoprotein is a major inhibitor of axonal regeneration in the CNS. Neuron 15:1375–1381.
Cai D, Shen Y, De Bellard M, Tang S, Filbin MT (1999) Prior exposure to neurotrophins blocks inhibition of axonal regeneration by MAG and myelin via a cAMP-dependent mechanism. Neuron 22:89–101.
Carim-Todd L, Escarceller M, Estivill X, Sumoy L (2003) LRRN6A/LERN1 (leucine-rich repeat neuronal protein 1), a novel gene with enriched expression in limbic system and neocortex. Eur J Neurosci 18:3167–3182.
Chivatakarn O, Venkatesh K, Lee H, Giger RJ (2004) The pan-neurotrophin receptor $p75^{NTR}$ is not necessary for MAG inhibition. Soc Neurosci Abstr 30:942.9.
Collins BE, Yang LJ, Mukhopadhyay G, Filbin MT, Kiso M, Hasegawa A, Schnaar RL (1997) Sialic acid specificity of myelin-associated glycoprotein binding. J Biol Chem 272:12148–1255.
Crocker PR, Varki A (2001) Siglecs, sialic acids and innate immunity. Trends Immunol 22:337–342.
DeBellard ME, Filbin MT (1999) Myelin-associated glycoprotein MAG selectively binds several neuronal proteins. J Neurosci Res 56:213–218.
DeBellard ME, Tang S, Mukhopadhyay G, Shen YJ, Filbin MT (1996) Myelin-associated glycoprotein inhibits axonal regeneration from a variety of neurons via interaction with a sialoglycoprotein. Mol Cell Neurosci 7:89–101.
Domeniconi M, Cao Z, Spencer T, Sivasankaran R, Wang K, Nikulina E, Kimura N, Cai H, Deng K, Gao Y, He Z, Filbin M (2002) Myelin-associated glycoprotein interacts with the Nogo-66 receptor to inhibit neurite outgrowth. Neuron 35:283–290.
Filbin MT (2003) Myelin-associated inhibitors of axonal regeneration in the adult mammalian CNS. Nat Rev Neurosci 4:703–713.
Fournier AE, GrandPre T, Strittmatter SM (2001) Identification of a receptor mediating Nogo-66 inhibition of axonal regeneration. Nature 409:341–346.
Fournier AE, Gould GC, Liu BP, Strittmatter SM (2002) Truncated soluble Nogo receptor binds Nogo-66 and blocks inhibition of axon growth by myelin. J Neurosci 22:8876–8883.
Franzen R, Tanner SL, Dashiell SM, Rottkamp CA, Hammer JA, Quarles RH (2001) Microtubule-associated protein 1B: a neuronal binding partner for myelin-associated glycoprotein. J Cell Biol 155:893–898.
Giger RJ, Wolfer DP, De Wit GM, Verhaagen J (1996) Anatomy of rat semaphorin III/collapsin-1 mRNA expression and relationship to developing nerve tracts during neuroembryogenesis. J Comp Neurol 375:378–392.
Giger RJ, Ziegler U, Hermens WT, Kunz B, Kunz S, Sonderegger P (1997) Adenovirus-mediated gene transfer in neurons: construction and characterization of a vector for heterologous expression of the axonal cell adhesion molecule axonin-1. J Neurosci Methods 71:99–111.
Giger RJ, Urquhart ER, Gillespie SKH, Levengood DV, Ginty DD, Kolodkin AL (1998) Neuropilin-2 is a receptor for semaphorin IV: insight into the structural basis of receptor function and specificity. Neuron 21:1079–1092.
Guirland C, Suzuki S, Kojima M, Lu B, Zheng JQ (2004) Lipid rafts mediate chemotropic guidance of nerve growth cones. Neuron 42:51–62.
Hasegawa Y, Fujitani M, Hata K, Tohyama M, Yamagishi S, Yamashita T (2004) Promotion of axon regeneration by myelin-associated glycoprotein and Nogo through divergent signals downstream of G_i/G. J Neurosci 24:6826–6832.
Hatten ME (1985) Neuronal regulation of astroglial morphology and proliferation *in vitro*. J Cell Biol 100:384–396.
Johnson PW, Abramow-Newerly W, Seilheimer B, Sadoul R, Tropak MB, Arquint M, Dunn RJ, Schachner M, Roder JC (1989) Recombinant myelin-associated glycoprotein confers neural adhesion and neurite outgrowth function. Neuron 3:377–385.
Kelm S, Pelz A, Schauer R, Filbin MT, Tang S, de Bellard ME, Schnaar RL, Mahoney JA, Hartnell A, Bradfield P, Crocker PR (1994) Sialoadhesin, myelin-associated glycoprotein, and CD22 define a new family of sialic acid-dependent adhesion molecules of the immunoglobulin superfamily. Curr Biol 4:965–972.
Klinger M, Taylor JS, Oertle T, Schwab ME, Stuermer CA, Diekmann H (2003) Identification of Nogo-66 receptor (NgR) and homologous genes in fish. Mol Biol Evol 21:76–85.
Kolodkin AL, Levengood DV, Rowe EG, Tai YT, Giger RJ, Ginty DD (1997) Neuropilin is a semaphorin III receptor. Cell 90:753–762.
Lauren J, Airaksinen MS, Saarma M, Timmusk T (2003) Two novel mammalian Nogo receptor homologs differentially expressed in the central and peripheral nervous systems. Mol Cell Neurosci 24:581–594.
Li W, Walus L, Rabacchi SA, Jirik A, Chang E, Schauer J, Zheng BH, Benedetti NJ, Liu BP, Choi E, Worley D, Silvian L, Mo W, Mullen C, Yang W, Strittmatter SM, Sah DW, Pepinsky B, Lee DH (2004) A neutralizing anti-Nogo66 receptor monoclonal antibody reverses inhibition of neurite outgrowth by central nervous system myelin. J Biol Chem 279:43780–43788.
Liu BP, Fournier A, GrandPre T, Strittmatter SM (2002) Myelin-associated glycoprotein as a functional ligand for the Nogo-66 receptor. Science 297:1190–1193.
Maasho K, Marusina A, Reynolds NM, Coligan JE, Borrego F (2004) Efficient gene transfer into the human natural killer cell line, NKL, using the Amaxa nucleofection system. J Immunol Methods 284:133–140.
McGee AW, Strittmatter SM (2003) The Nogo-66 receptor: focusing myelin inhibition of axon regeneration. Trends Neurosci 26:193–198.
McKerracher L, David S, Jackson DL, Kottis V, Dunn RJ, Braun PE (1994) Identification of myelin-associated glycoprotein as a major myelin-derived inhibitor of neurite growth. Neuron 13:805–811.
Mi S, Lee X, Shao Z, Thill G, Ji B, Relton J, Levesque M, Allaire N, Perrin S, Sands B, Crowell T, Cate RL, McCoy JM, Pepinsky RB (2004) LINGO-1 is a component of the Nogo-66 receptor/p75 signaling complex. Nat Neurosci 7:221–228.
Mukhopadhyay G, Doherty P, Walsh FS, Crocker PR, Filbin MT (1994) A novel role for myelin-associated glycoprotein as an inhibitor of axonal regeneration. Neuron 13:757–767.
Niederost B, Oertle T, Fritsche J, McKinney RA, Bandtlow CE (2002) Nogo-A and myelin-associated glycoprotein mediate neurite growth inhibition by antagonistic regulation of RhoA and Rac1. J Neurosci 22:10368–10376.
Norton WT, Poduslo SE (1973) Myelination in rat brain: method of myelin isolation. J Neurochem 21:749–757.
Oertle T, van der Haar ME, Bandtlow CE, Robeva A, Burfeind P, Buss A, Huber AB, Simonen M, Schnell L, Brösamle C, Kaupmann K, Vallon R, Schwab ME (2003) Nogo-A inhibits neurite outgrowth and cell spreading with three discrete regions. J Neurosci 23:5393–5406.
Pignot V, Hein AE, Barske C, Wiessner C, Walmsley AR, Kaupmann K, Mayeur H, Sommer B, Mir AK, Frentzel S (2003) Characterization of two novel proteins, NgRH1 and NgRH2, structurally and biochemically homologous to the Nogo-66 receptor. J Neurochem 85:717–728.
Popkov M, Mage RG, Alexander CB, Thundivalappil S, Barbas 3rd CF, Rader C (2003) Rabbit immune repertoires as sources for therapeutic monoclonal antibodies: the impact of kappa allotype-correlated variation in cysteine content on antibody libraries selected by phage display. J Mol Biol 325:325–335.
Schachner M, Bartsch U (2000) Multiple functions of the myelin-associated glycoprotein MAG (Siglec-4a) in formation and maintenance of myelin. Glia 29:154–165.
Schafer M, Fruttiger M, Montag D, Schachner M, Martini R (1996) Disruption of the gene for the myelin-associated glycoprotein improves axonal regrowth along myelin in C57BL/Wlds mice. Neuron 16:1107–1113.
Schwab ME, Kapfhammer JP, Bandtlow CE (1993) Inhibitors of neurite growth. Annu Rev Neurosci 16:565–595.
Sben YJ, DeBellard ME, Salzer JL, Roder J, Filbin MT (1998) Myelin-associated glycoprotein in myelin and expressed by Schwann cells inhibits axonal regeneration and branching. Mol Cell Neurosci 12:79–91.
Sicotte M, Tsatas O, Jeong SY, Cai CQ, He Z, David S (2003) Immunization with myelin or recombinant Nogo-66/MAG in alum promotes axon regeneration and sprouting after corticospinal tract lesions in the spinal cord. Mol Cell Neurosci 23:251–263.
Song XY, Zhong JH, Wang X, Zhou XF (2004) Suppression of p75NTR does not promote regeneration of injured spinal cord in mice. J Neurosci 24:542–546.
Strenge K, Schauer R, Kelm S (1999) Binding partners for the myelin-associated glycoprotein of N2A neuroblastoma cells. FEBS Lett 444:59–64.
Strenge K, Brossmer R, Ihrig P, Schauer R, Kelm S (2001) Fibronectin is a binding partner for the myelin-associated glycoprotein (Siglec-4a). FEBS Lett 499:262–267.
Sun J, Shaper NL, Itonori S, Heffer-Lauc M, Sheikh KA, Schnaar RL (2004) Myelin-associated glycoprotein (Siglec-4) expression is progressively and

selectively decreased in the brains of mice lacking complex gangliosides. Glycobiology 14:851–857.

Tang S, Shen YJ, DeBellard ME, Mukhopadhyay G, Salzer JL, Crocker PR, Filbin MT (1997) Myelin-associated glycoprotein interacts with neurons via a sialic acid binding site at ARG118 and a distinct neurite inhibition site. J Cell Biol 138:1355–1366.

Trapp BD, Andrews SB, Cootauco C, Quarles R (1989) The myelin-associated glycoprotein is enriched in multivesicular bodies and periaxonal membranes of actively myelinating oligodendrocytes. J Cell Biol 109:2417–2426.

Tsui-Pierchala BA, Encinas M, Milbrandt J, Johnson Jr EM (2002) Lipid rafts in neuronal signaling and function. Trends Neurosci 25:412–417.

Umemori H, Sato S, Yagi T, Aizawa S, Yamamoto T (1994) Initial events of myelination involve Fyn tyrosine kinase signaling. Nature 367:572–576.

Vinson M, Strijbos PJ, Rowles A, Facci L, Moore SE, Simmons DL, Walsh FS (2001) Myelin-associated glycoprotein interacts with ganglioside GT1b. A mechanism for neurite outgrowth inhibition. J Biol Chem 276:20280–20285.

Vinson M, Rausch O, Maycox PR, Prinjha RK, Chapman D, Morrow R, Harper AJ, Dingwall C, Walsh FS, Burbidge SA, Riddell DR (2003) Lipid rafts mediate the interaction between myelin-associated glycoprotein (MAG) on myelin and MAG-receptors on neurons. Mol Cell Neurosci 22:344–352.

Vyas AA, Schnaar RL (2001) Brain gangliosides: functional ligands for myelin stability and the control of nerve regeneration. Biochem J 83:677–682.

Vyas AA, Patel HV, Fromholt SE, Heffer-Lauc M, Vyas KA, Dang J, Schachner M, Schnaar RL (2002) Gangliosides are functional nerve cell ligands for myelin-associated glycoprotein (MAG), an inhibitor of nerve regeneration. Proc Natl Acad Sci USA 99:8412–8417.

Walmsley AR, McCombie G, Neumann U, Marcellin D, Hillenbrand R, Mir AK, Frentzel S (2004) Zinc metalloproteinase-mediated cleavage of the human Nogo-66 receptor. J Cell Sci 117:4591–4602.

Wang KC, Koprivica V, Kim JA, Sivasankaran R, Guo Y, Neve RL, He Z (2002a) Oligodendrocyte-myelin glycoprotein is a Nogo receptor ligand that inhibits neurite outgrowth. Nature 417:941–944.

Wang KC, Kim JA, Sivasankaran R, Segal R, He Z (2002b) p75 interacts with the Nogo receptor as a co-receptor for Nogo, MAG, and OMgp. Nature 420:74–78.

Wang X, Chun S, Treloar H, Vartanian T, Greer CA, Strittmatter SM (2002) Localization of Nogo-A and Nogo-66 receptor proteins at sites of axon–myelin and synaptic contact. J Neurosci 22:5505–5515.

Wong ST, Henley JR, Kanning KC, Huang KH, Bothwell M, Poo MM (2002) A $p75^{NTR}$ and Nogo receptor complex mediates repulsive signaling by myelin-associated glycoprotein. Nat Neurosci 5:1302–1308.

Yamashita T, Higuchi H, Tohyama M (2002) The p75 receptor transduces the signal from myelin-associated glycoprotein to Rho. J Cell Biol 157:565–570.

Yang LJ, Zeller CB, Shaper NL, Kiso M, Hasegawa A, Shapiro RE, Schnaar RL (1996) Gangliosides are neuronal ligands for myelin-associated glycoprotein. Proc Natl Acad Sci USA 93:814–818.

THE JOURNAL OF BIOLOGICAL CHEMISTRY VOL. 282, NO. 8, pp. 5715–5725, February 23, 2007

Characterization of Myelin Ligand Complexes with Neuronal Nogo-66 Receptor Family Members*[S]

Received for publication, October 17, 2006 Published, JBC Papers in Press, December 21, 2006, DOI 10.1074/jbc.M609797200

Juha Laurén‡, Fenghua Hu‡, Joanna Chin‡, Ji Liao‡, Matti S. Airaksinen§, and Stephen M. Strittmatter‡1

From the ‡Departments of Neurology and Neurobiology, Yale University School of Medicine, New Haven, Connecticut 06520 and the §Neuroscience Center, University of Helsinki, FIN-00014 Helsinki, Finland

Nogo, MAG, and OMgp are myelin-associated proteins that bind to a neuronal Nogo-66 receptor (NgR/NgR1) to limit axonal regeneration after central nervous system injury. Within Nogo-A, two separate domains are known interact with NgR1. NgR1 is the founding member of the three-member NgR family, whereas Nogo-A (RTN4A) belongs to a four-member reticulon family. Here, we systematically mapped the interactions between these superfamilies, demonstrating novel nanomolar interactions of RTN2 and RTN3 with NgR1. Because RTN3 is expressed in spinal cord white matter, it may have a role in myelin inhibition of axonal growth. Further analysis of the Nogo-A and NgR1 interactions revealed a novel third interaction site between the proteins, suggesting a trivalent Nogo-A interaction with NgR1. We also confirmed here that MAG binds to NgR2, but not to NgR3. Unexpectedly, we found that OMgp interacts with MAG with a higher affinity compared with NgR1. To better define how these multiple structurally distinct ligands bind to NgR1, we examined a series of Ala-substituted NgR1 mutants for ligand binding activity. We found that the core of the binding domain is centered in the middle of the concave surface of the NgR1 leucine-rich repeat domain and surrounded by differentially utilized residues. This detailed knowledge of the molecular interactions between NgR1 and its ligands is imperative when assessing options for development of NgR1-based therapeutics for central nervous system injuries.

When nerve fibers of the brain and spinal cord in adult mammals are severed, little to no regrowth occurs. Astroglial scarring and central nervous system myelin pose extrinsic barriers to regeneration (1, 2). From central nervous system myelin, at least three proteins capable of inhibiting axonal growth *in vitro* are recognized: Nogo-A, MAG, and OMgp (1, 2). Nogo-A has several domains that participate in inhibiting axonal growth. The hydrophilic Nogo-66 domain flanked by two hydrophobic segments is detectable on the oligodendrocyte surface (3, 4). Together, these three segments form a reticulon (RTN)[2] homology domain (RHD) of ~200 amino acids, characteristic of reticulon family members (5).

Nogo-66 binding provided the basis for the identification of a Nogo-A receptor (NgR/NgR1) (6). Remarkably, MAG and OMgp also bind to NgR1 to inhibit axonal growth *in vitro* (7–9). NgR1 is a leucine-rich repeat (LRR)-containing glycosylphosphatidylinositol-anchored neuronal protein; the structure of its LRR domain has been determined (10, 11).

Perturbation of Nogo function by antibodies (12–14), peptide, or the soluble NgR1 ectodomain (15–19) leads to enhanced axonal growth, plasticity, and functional recovery after spinal injury or stroke. Genetic studies of Nogo-A (20–22) and NgR1 (23, 24) have, however, found less clear-cut evidence of their role in axonal regeneration. It is plausible that adaptive compensation for chronic genetic loss of NgR1 or Nogo-A may explain this observation in part.

Alternatively, the less pronounced genetic *versus* pharmacological phenotype might relate to redundancy among the myelin inhibitory proteins and their signaling pathways. NgR1 is the founding member of the three-member NgR family (11, 25, 26); Nogo-A belongs to a four-member RTN family (5). MAG and OMgp have no known paralogs. A recent report demonstrated that, *in vitro*, MAG can bind and exert its inhibitory function via NgR2 as well as NgR1 (27). The ability of OMgp to bind other NgR family members has not been assessed. The functions of other RTNs are largely enigmatic (28). As other RTNs are also present in the central nervous system and contain homologous RHDs, we hypothesized previously that they could interact with NgR family members (25). Here, we have mapped the NgR family binding properties of all RTNs, MAG, and OMgp. We also demonstrate that RTN3, which we found to bind to NgR1, is expressed in spinal cord white matter.

Several topologies of Nogo-A relative to the lipid bilayer have been supported experimentally. The extended length, 35 and 36 amino acids (3), of the hydrophobic segments flanking the Nogo-66 segment suggests that these segments might not be single-pass transmembrane regions. A recent report supports the existence of a conformation in which all three of the hydrophilic segments of the RTNs are on the same side of the lipid bilayer (29). This raises the possibility that C-terminal amino

* This work was supported by National Institutes of Health Grants NS42304 and NS39962 and Biogen Idec (to S. M. S.). The costs of publication of this article were defrayed in part by the payment of page charges. This article must therefore be hereby marked "*advertisement*" in accordance with 18 U.S.C. Section 1734 solely to indicate this fact.

[S] The on-line version of this article (available at http://www.jbc.org) contains supplemental Figs. 1 and 2 and Ref. 1.

1 To whom correspondence should be addressed: Dept. of Neurology, Yale University School of Medicine, 333 Cedar St., New Haven, CT 06520. Tel.: 203-785-4878; Fax: 203-785-5098; E-mail: stephen.strittmatter@yale.edu.

2 The abbreviations used are: RTN, reticulon; RHD, reticulon homology domain; NgR, Nogo-66 receptor; LRR, leucine-rich repeat; AP, alkaline phosphatase.

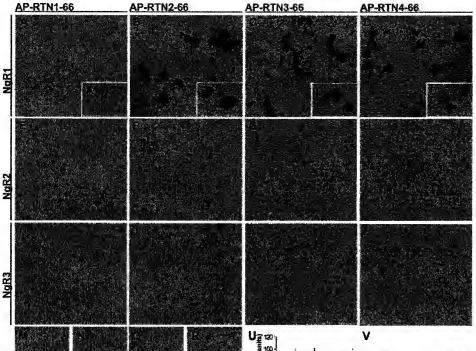

FIGURE 1. **Analysis of interactions between RTN family and LRR-containing protein superfamily members shows that RTN2-66 and RTN3-66 interact specifically with NgR1.** RTN1-66 at either 6 nM (*A*) or 3 nM (*A′*) did not bind to NgR1, whereas 6 nM RTN2-66 (*B*), RTN3-66 (*C*), and RTN4-66/Nogo-66 (*D*) showed strong binding. Similarly, binding of 3 nM RTN2-66 (*B′*), RTN3-66 (*C′*), and RTN4-66 (*D′*) was clearly detectable. No binding of RTN1–4-66 at 50 nM to NgR2 (*E–H*, respectively) or to NgR3 (*I–L*, respectively) was detectable. None of the RTNs bound at 50 nM to other members of the LRR-containing protein superfamily tested: Lingo-1 (*M–P*, respectively) and TLR4 (*Q–T*, respectively). The dissociation constants for RTN1–4-66 interactions with NgR1 were determined (*U*). A summary of the K_d values for RTN1–4-66/NgR1 interactions (means ± S.E. from five experiments) is presented (*V*), as is a sequence alignment of the mouse RTN1–4 66-amino acid loop regions (*W*). *mm*, *Mus musculus*. Identical amino acids are indicated with *asterisks*; high physicochemical similarity of amino acids is indicated with *colons* and similarity with *periods*. In RTN4, the amino-terminal half (*underlined*) is indispensable for receptor binding. Non-conserved amino acids are highlighted in *yellow*, and putative residues in RTN1-66 responsible for the lost NgR1 affinity are highlighted in *red*. *Scale bars* = 100 μm (*D* and *T*).

acids might contribute to NgR1 binding, a hypothesis we test here.

The molecular basis for NgR1 interaction with multiple ligands has not been defined. LRR domains are commonly involved in protein/protein interactions presumably because the non-globular extended surface of the LRR domain provides ample opportunities for high affinity interactions. Here, we show that NgR1 utilizes certain residues to interact with multiple ligands in a central binding region and other surrounding residues to interact with specific ligands. These data helps us to understand the ligand specificity of different NgR family members and contribute to the elucidation of how central nervous system axonal plasticity and regeneration are limited by the interaction between multiple ligands and NgR family members.

EXPERIMENTAL PROCEDURES

Recombinant DNA Constructs—The alkaline phosphatase (AP)-Nogo-66, AP-Y4C (human Nogo-A amino acids 950–1018), AP-Nogo-A-24 (human Nogo-A amino acids 995–1018) AP-MAG, AP-OMgp, and AP-Lingo-1 constructs have been described (6, 8, 9, 30, 31). To generate additional AP fusion proteins, DNA fragments encoding 66-amino acid sequences of RTN1, RTN2, and RTN3 (as shown in Fig. 1*W*) were cloned into pAPtag5 (kindly provided by Dr. J. G. Flanagan, Harvard Medical School) (32) with restriction enzyme XbaI. For the AP-C-terminal Nogo-A construct (AP-Nogo-C39), the DNA encoding the last 39 amino acids of human Nogo-A was cloned into the XbaI site of pAPtag5. An additional MAG-AP construct was generated by cloning the sequence encoding the MAG ectodomain devoid of signal peptide into the HindIII and BglII restriction sites in pAPtag5. Mouse MAG, TLR4, NgR2, and NgR3 expression constructs contain Igκ signal peptide and Myc and His_6 tags, followed by respective open reading frames devoid of signal peptides. These inserts were cloned into the XbaI restriction site of a modified pSecTag2a plasmid in which the stop codon was replaced with the XbaI site. pSecTag2a was modified using the QuikChange II site-directed mutagenesis kit (Stratagene). The Myc-NgR1 expression construct has been described (6). Also, an additional AP-Nogo-66 construct based on the pAPtag5 plasmid backbone was used in some experiments. This was created by subcloning an insert from the original pcAP-5-Nogo-66 plasmid (6) into the pAPtag5 vector. All constructs were sequenced to confirm that no unwanted changes had occurred.

NgR1 Mutagenesis—NgR1 mutagenesis was accomplished using the QuikChange multisite-directed mutagenesis kit (Stratagene). A FLAG-tagged human NgR1 expression construct was used as a template. All mutant NgR1 constructs were analyzed by sequencing.

Recombinant Proteins—Expression vectors encoding AP fusion proteins were transfected into HEK293T cells, and conditioned media were collected after 5–7 days. In some cases, conditioned media were concentrated using Amicon Ultra centrifugal filtration devices (Millipore Corp.). His_6 tag-containing

AP-MAG, MAG-AP, and AP-OMgp were purified from conditioned media using nickel-nitrilotriacetic acid affinity resin (Qiagen Inc.) according to the manufacturer's guidelines.

COS-7 Ligand Binding Assay—COS-7 binding assays were performed as described (6). Conditioned media containing AP-fused ligands or purified ligands were incubated with COS-7 cells transfected with the indicated constructs for 1–2 h at room temperature before washing and fixation. Bound AP was visualized by 5-bromo-4-chloro-3-indolyl phosphate/nitro blue tetrazolium reaction.

Immunocytochemistry—Live cell immunostaining was performed by incubating cells in Hanks' balanced saline solution with 0.05% bovine serum albumin and AP-conjugated anti-Myc antibody (9E10, Sigma; 1:200 dilution) or anti-NgR1 antibody (6) at room temperature or on ice for 1 h, followed by washing and fixation. The cells were then incubated for 1.5 h in 65 °C. Finally, bound antibodies were visualized by 5-bromo-4-chloro-3-indolyl phosphate/nitro blue tetrazolium reaction.

In Situ Hybridization—*In situ* hybridization was performed as described (25). The RTN probes described previously (25) were designed to recognize the splice variants containing the sequence encoding the 66-amino acid loop region.

RESULTS

NgR1 Is a High Affinity Receptor for Several RTN Family Members—We prepared N-terminal AP fusion proteins of all RTN 66-amino acid loop regions and analyzed their binding properties for NgR family members (Fig. 1). We found that, in addition to Nogo-66, RTN2-66 and RTN3-66 interact with NgR1, but not with other NgR family members or other related members of the type I transmembrane LRR-containing protein superfamily tested (Fig. 1). The affinities of RTN2-66, RTN3-66, and Nogo-66 for NgR1 appeared to be similar, with K_d values for RTN2-66 and Nogo-66 of ~1 nM and for RTN3-66 of ~4 nM (Fig. 1*V*). RTN1-66 showed no affinity for NgR1 even at the highest concentration tested (50 nM).

Rtn3 and Nogo-A Are Expressed in the Same Glial Cell Population of Spinal Cord White Matter—A previous report showed Nogo-A expression in central nervous system oligodendrocytes (4). However, the possible expression of other RTNs in spinal cord white matter has not been analyzed. We analyzed the expression of all RTN mRNAs in adult mouse lumbar spinal cord by *in situ* hybridization. Consistent with the previous study (25), we found that all RTN mRNAs were expressed in neurons (Fig. 2). Interestingly, we found prominent expression of *Rtn3* and *Rtn4* mRNA transcripts in the white matter/lateral funiculus (Fig. 2, *I* and *L*, *arrowheads*). Nissl counterstaining of the sections enabled large and weakly stained nuclei (neurons) to be distinguished from small and strongly stained nuclei (glia). We noted that glial cell nuclei of the stained cryosections displayed dichotomy in size distribution and that Nogo-A and *Rtn3* mRNAs were expressed by the same cell population characterized by larger and more weakly stained nuclei compared with other glial cells. The probes used in these experiments were designed to cover the conserved RHDs and are relatively homologous: in the most homologous 203-nucleotide sequence stretch, *Rtn3* and Nogo-A probes are 73% identical, but contain no identical nucleotide stretches longer than 11 nucleotides. Notably, in the Purkinje cell layer of the cerebellum, strong Nogo-A mRNA expression was observed, but no or low level expression of *Rtn3* mRNA was detected, thus confirming the specificity of the hybridization reaction (supplemental Fig. 1). No signal was detected with control sense probes (data not shown).

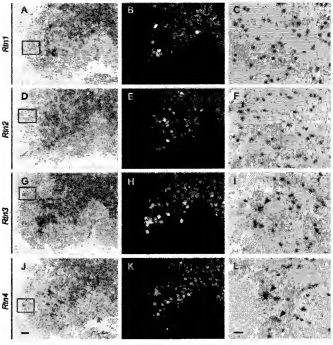

FIGURE 2. **Rtn3 and *Rtn4* (Nogo-A) mRNAs, but not *Rtn1* and *Rtn2* mRNAs, are expressed in adult mouse spinal cord white matter.** We analyzed the localization of the *Rtn1* (*A–C*), *Rtn2* (*D–F*), *Rtn3* (*G–I*), and *Rtn4* (*J–L*) mRNAs in adult mouse lumbar spinal cord by *in situ* hybridization. Prominent expression of all four transcripts was observed in neuronal cells in gray matter. Furthermore, *Rtn3* and *Rtn4* mRNAs were detected in non-neuronal cells (*A*, *D*, *G*, and *J*, *boxed areas*). *C*, *F*, *I*, and *L* are the *boxed areas* in *A*, *D*, *G*, and *J*, respectively, at higher magnification and show prominent *Rtn3* and *Rtn4* signals and that the signals overlap with non-neuronal cells with relatively larger nuclei (*red arrowheads*). *Scale bars* = 100 μm (*J*, for lower magnification images) and 20 μm (*L*, for higher magnification images).

Nogo-A Interaction with NgR1 Involves Three Segments of Nogo-A—We produced an AP fusion protein of the C-terminal 39 residues of Nogo-A (AP-Nogo-C39) and measured its affinity for NgR family members. We found that it interacted with high affinity and specificity with only NgR1 (Fig. 3). The NgR1 binding affinity (K_d) of AP-Nogo-C39 was determined to be nearly the same as that of the AP-Nogo-A-24 fragment; however, AP-Nogo-66 showed the highest affinity for NgR1. We also reconsidered the K_d of the Nogo-66/NgR1 interaction. The AP-Nogo-66 protein we used in previous studies was found to have been proteolytically cleaved to a significant degree between the AP moiety and Nogo-66. Re-subcloning of the same insert into the pAPtag5 plasmid serendipitously led to formation of a stable recombinant protein (supplemental Fig. 2). This allowed us to determine Nogo-66 affinity for NgR1 more accurately than in previous studies and suggests that partial ligand degradation is likely to have resulted in an underestimation of Nogo-66 affinity for NgR1. We concluded that Nogo-66 binds to NgR1 with a K_d of 1 nM.

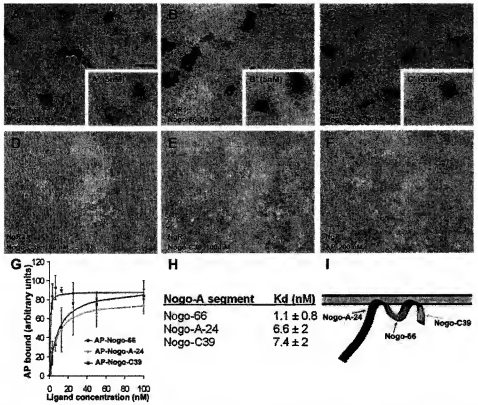

FIGURE 3. **The C-terminal segment of Nogo-A (Nogo-C39) binds to NgR1, but not to other NgR family members.** 50 nM (*A*) and 5 nM (*A'*) Nogo-C39, 50 nM (*B*) and 5 nM (*B'*) Nogo-66, and 50 nM (*C*) and 5 nM (*C'*) Nogo-A-24 all bound to NgR1 with high affinity. No interaction of Nogo-C39 with NgR2 (*D*) or with NgR3 (*E*) was detected. AP protein alone showed no affinity for NgR1 even at high concentration (200 nM) (*F*). The dissociation constants for interactions between different Nogo-A fragments and NgR1 were determined (*G*). Data were averaged from three experiments. A summary of the K_d values for the interactions (means ± S.E.) is provided (*H*). A schematic drawing (N terminus not drawn to scale) highlighting the different NgR1-binding segments of Nogo-A is shown (*I*). *Scale bar* = 100 μm (*A*).

The C-terminal Fragment of Nogo-A Interacts Exclusively with the LRR Domain of NgR1—We mapped the interaction site of Nogo-C39 in NgR1 using a series of deletion mutants lacking pairs of the LRR or other structural elements in NgR1 as described (33). The LRR domain of NgR1 was indispensable for Nogo-C39 binding (Fig. 4).

MAG Binds to NgR1 and NgR2 with Moderate Affinity and Shows No Affinity for NgR3—Venkatesh *et al.* (27) reported that MAG-Fc interacts with NgR2 and that NgR2 mediates MAG-dependent growth inhibitory signaling other than NgR1-mediated signaling. Previously, we failed to observe AP-MAG fusion protein binding to human NgR2 (11). As Venkatesh *et al.* also failed to see AP-MAG/NgR2 interaction, they proposed that AP tagging of MAG sterically interferes with the binding to NgR2, but not to NgR1. Since then, we have identified a non-conservative nucleotide variant in the PCR-derived NgR2 expression construct used in our previous study. When using a wild-type NgR2 expression plasmid, we found that AP-MAG bound with similar affinity to NgR2 and NgR1 (Fig. 5). Because of the higher expression level of the transfected Myc-NgR2 construct, we observed higher maximal binding of AP-MAG to NgR2- than to NgR1-expressing cells. However, as analyzed by Scatchard analysis, the dissociation constants for these interactions were essentially identical using these constructs. MAG had no detectable affinity for NgR3. Binding experiments using MAG-AP resulted in similar results (data not shown).

OMgp Binds MAG with Very High Affinity and NgR1 with Moderate Affinity and Does Not Interact with NgR2 or NgR3—OMgp was identified previously as a myelin inhibitory molecule interacting with NgR1 (9). To investigate whether OMgp can also interact with NgR2 or NgR3, we prepared AP-OMgp recombinant protein and assessed its affinity for NgR family members. As reported previously (9), we found that OMgp interacted with NgR1. Unexpectedly, under other conditions tested, we found that OMgp interacted with MAG and that this interaction had significantly higher affinity than the binding affinity of OMpg/NgR1 interaction. The K_d values for OMgp/MAG and OMgp/NgR1 interactions are 3–6 and 10–20 nM, respectively (Fig. 5, *J* and *K*) (data not shown). We did not detect OMgp binding to NgR2 or NgR3 (data not shown).

A Library of NgR1 Mutants Is Expressed in a Similar Fashion Compared with Wild-type NgR1—NgR1 has the capacity to bind Nogo-66, MAG, OMgp, Lingo-1, Nogo-A-24 and Nogo-C39 (6–9, 31). To better define how multiple ligands with so wide a structural diversity bind to NgR1, we examined a series of Ala-substituted NgR1 mutants for ligand binding activity. An Ala substitution was generated for each of the charged residues predicted to be solvent-accessible at the surface of the ligand-binding LRR domain of NgR1 (10, 11). We generated mutants in which 1–8 surface residues localized within 5 Å of one another were Ala-substituted. Because of the coiling nature of the LRR structure, residues juxtaposed on the protein surface are separated by ~25 residues in the primary structure. In addition to mutations in specific charged surface patches, other mutations were targeted to glycosylation sites (Asn^{82} and Asn^{179}) and to regions predicted to be involved in ligand binding based on the NgR1 structure (10, 11). A variant corresponding to a human polymorphism present in the GenBank™ Data Bank was also examined (D259N). None of the mutations altered the Leu residues critical for the tertiary LRR structure or the Cys residues involved in disulfide bond formation in the N- and C-terminal capping domains. The vast majority of such surface Ala-substituted mutants were expressed as immunoreactive polypeptides with molecular masses and expression levels indistinguishable from those wild-type NgR1 (Fig. 6*A*) (data not shown). Those that where not expressed were excluded from further analysis. Moreover, all of the NgR1 mutants that

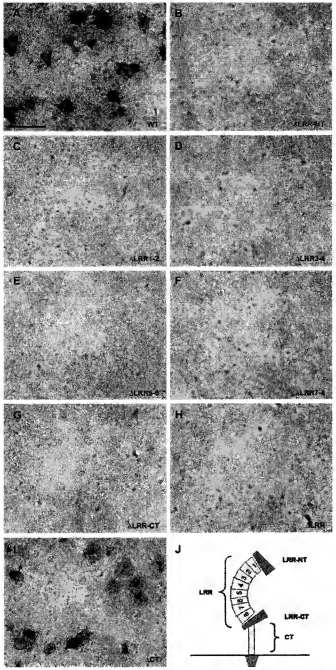

FIGURE 4. **The LRR domain of NgR1 is necessary for binding of the C-terminal segment of Nogo-A.** Binding of Nogo-C39 at 50 nM to full-length wild-type (*WT*) NgR1 (*A*), deletion mutants lacking the indicated LRR units (*C–H*), adjacent cysteine-rich flanking regions (N-terminal (*LRR-NT*) and C-terminal (*LRR-CT*); *B* and *G*), or the juxtamembrane stalk region (*CT*; *I*) was detected. Different structural units are indicated in *J*. All NgR1 deletion constructs were detected on the plasma membrane by live cell staining with anti-FLAG antibody (data not shown) (33). *Scale bar* = 100 μm (*A*).

were analyzed for ligand binding exhibited a cellular distribution in transfected COS-7 identical to that of the wild-type protein (Fig. 6*B*) (data not shown). Notably, those mutations that removed both glycosylation sites in the LRR domain (amino acids 82 and 179) did not alter expression levels or surface localization, although the molecular masses were reduced as determined by immunoblot analysis (data not shown).

Myelin Ligand Binding to NgR1 Requires Overlapping but Separate Residues—We used the library of 74 NgR1 mutants to test for their AP-Nogo-66, AP-Nogo-Y4C, AP-Nogo-C39, AP-MAG, AP-OMgp, and AP-Lingo-1 binding abilities. The properties of the NgR1 mutants fall into one of three major categories (Fig. 7*B* and Table 1). A number of Ala-substituted NgR1 variants bound all of the ligands at wild-type levels. We concluded that the corresponding residues do not play an essential role in ligand interactions. Many of these residues are situated on the convex side of the NgR1 structure, indicating that this surface is not a primary site for these interactions. In addition, a significant extent of the concave surface is dispensable for ligand binding. Glycosylation at residue 179 is not essential for ligand binding. The D259N polymorphic variant exhibited normal ligand binding properties (Table 1).

A second group of mutants exhibited weak or no binding to each of the ligands (Fig. 7*B* and Table 1). One interpretation is that these residues are required for NgR1 folding, so their substitution with Ala results in misfolded protein with no ligand binding. However, there are several reasons to favor the alternative hypothesis that many of these residues contribute to the binding of multiple NgR1 ligands in a common binding pocket. Critically, the NgR1 expression levels and subcellular distribution were not altered for these mutants (data not shown). In contrast, misfolded proteins might be expected to be unstable and mislocalized. Notably, the majority of those residues that could not be mutated to Ala without losing affinity for all ligands are clustered near one another. Thus, we concluded that the NgR1 surface created by residues 67/68, 111/113, 133/136, 158/160, 163, 182/186, and 232/234 constitutes a primary binding site for these ligands. Mouse and human NgR1 are identical at all 13 of these positions, supporting a conserved functional role for these residues. Human and mouse NgR1 differ from human and mouse NgR2 at four of these positions (Arg/Leu at position 68, Ser/Lys at position 113, His/Gln at position 133, and Asp/Glu at position 163), whereas human and mouse NgR1 differ from human and mouse NgR3 at three of these positions (Ser/Gly at position 113, His/Tyr at position 136, and Tyr/Phe at position 232). The non-conservative changes at these sites may account for the inability of NgR2 and NgR3 to bind several ligands specific for NgR1. Removal of both NgR1 *N*-linked glycosylation sites (residues 82 and 179) abrogated binding to all ligands. Because the 82/179 mutant was expressed at the cell surface, the lack of binding indicates that glycosylation contributes to either protein folding or ligand binding directly.

The third group of Ala-substituted NgR1 mutants exhibited selective loss of binding for some ligands, but not others (Tables 1 and 2). The preservation of binding affinity for at least one ligand by each member of this class demonstrates that the Ala replacements do not prevent NgR1 folding and surface expression. Most of the NgR1 residues responsible for differential ligand binding are situated at the perimeter of the primary binding site described above. Many of these substitutions reduced or eliminated MAG, OMgp, and Lingo-1 binding without diminishing binding by Nogo-66, Nogo-Y4C, or Nogo-C39. The simplest interpretation of this topographic relationship is that MAG, OMgp, and Lingo-1 require not only a central ligand-binding domain that is partially shared with multiple

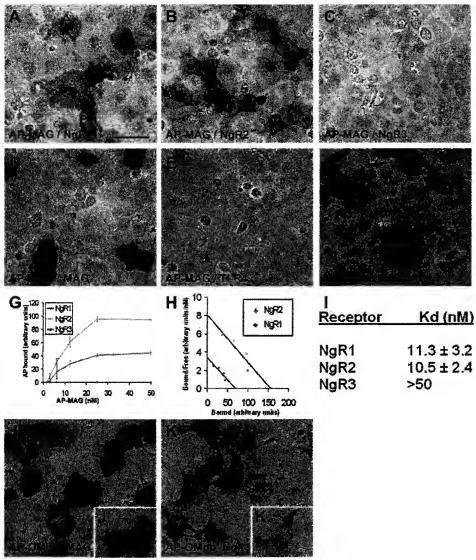

FIGURE 5. **Interactions between MAG, OMgp, and NgR family members.** 15 nM MAG bound avidly to NgR1 (*A*) and NgR2 (*B*), but not to NgR3 (*C*) or to another member of the LRR-containing protein superfamily, TLR4 (*E*). Homophilic binding of AP-MAG to MAG expressed on the cell surface was also detected (*D*). Cell-surface expression of Myc-NgR3 was confirmed by live cell staining with anti-Myc antibody (*F*). The results from analysis of MAG binding to NgRs as a function of ligand concentration are shown (*G*). Data are averaged from four experiments. The K_d values for MAG interaction with NgR1 and NgR2 were determined by Scatchard analysis (*H*). A summary of the K_d values for MAG/NgR interactions (means ± S.E.) is provided (*I*). AP-OMgp (25 nM (*J* and *K*) and 12 nM (*J'* and *K'*)) bound MAG with higher affinity compared with NgR1. *Scale bar* = 100 μm (*A*).

81, His/Tyr at position 89, Arg/Tyr at position 95, Asp/His at position 97, Ser/Thr at position 120, and Asp/Gly at position 259). Two of these changes are conservative (His/Tyr at position 89 and Ser/Thr at position 120); two are moderately conservative (Asp/His at position 97 and Asp/Gly at position 259); and three are non-conservative. The lack of amino acid conservation at these sites may account for the inability of NgR2 to bind OMgp and of NgR3 to bind MAG and OMgp.

Of special interest is the glycosylation site at residue 82. Mutating this glycosylation site to Ala reduced MAG, OMgp, and Lingo-1 binding. Interestingly, NgR2, which binds MAG, has a potential glycosylation site at Asn^{82}, whereas in NgR3, this has been naturally replaced with Ala, and concomitantly, affinity for MAG has been lost. This suggests that sugar moieties attached to Asn^{82} contribute to NgR1 interaction with these particular ligands. Consistent with this model, MAG interaction with neurons expressing NgR1 and NgR2 has been shown to be at least partially sialic acid-dependent, and both receptors have been shown to likely be highly sialylated glycoproteins (27).

All three Nogo-A fragments were found to interact with residues located on the central portion of the concave side of the LRR domain. We did not identify mutants that differentially displayed reduced affinity for a certain Nogo-A segment. However, it is possible that higher resolution mapping of NgR1 residues involved in ligand binding could reveal differences in their binding sizes.

NgR1-interacting Nogo-A fragments, but also an adjacent group of residues for high affinity binding. This adjacent region includes amino acids 78/81, 87/89, 89/90, 95/97, 108, 119/120, 139, 210, and 256/259. Mouse and human NgR1 are identical at 11 and similar at 13 of these 14 residues. Human NgR2 exhibits less conservation at these 14 positions, with 8 identical and 6 non-identical amino acids compared with human NgR1 (Arg/Gly at position 78, Arg/Ser at position 81, His/Phe at position 89, Arg/Thr at position 95, Asp/Tyr at position 97, and Asp/Ala at position 259). One of these changes is conservative (similar/non-identical amino acids; His/Phe at position 89), and five are non-conservative (dissimilar amino acids). For human NgR3, there are 7 identical and 7 non-identical amino acids compared with human NgR1 (Arg/Ser at position 78, Arg/Pro at position

DISCUSSION

This study has extended our understanding of how myelin inhibitors interact with NgR family members: NgR1 binds three linear segments of Nogo-A as well as MAG and OMgp; mutagenesis defined overlapping NgR1-binding sites for different ligands; RTN2 and RTN3 also bind NgR1 with high affinity; NgR2 binds MAG, but not RTNs; and finally, NgR3 binds none of the known NgR family ligands.

As all RTNs are also present in the central nervous system and as they all contain homologous 66-amino acid loop regions, we hypothesized previously that they could interact with

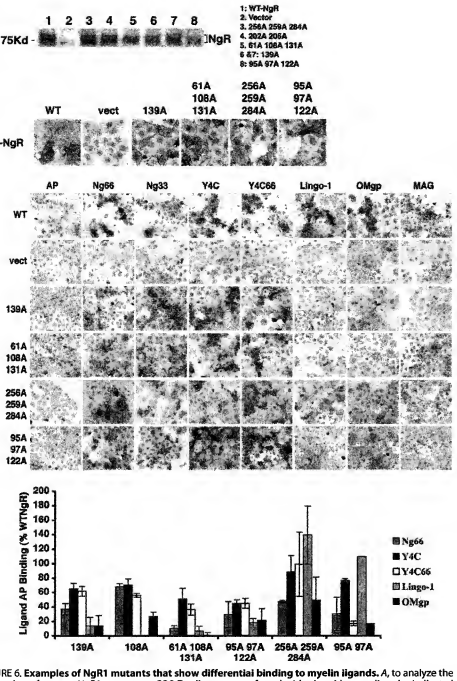

FIGURE 6. **Examples of NgR1 mutants that show differential binding to myelin ligands.** *A*, to analyze the expression of mutant NgR1 constructs, COS-7 cells were transfected with plasmids encoding the indicated constructs; lysates were subjected to SDS-PAGE; and Western blotting was performed with anti-NgR1 antibody. *B*, the indicated mutant NgR1 proteins were detected at the surface of transfected COS-7 cells by immunocytochemistry. Live COS-7 cells were incubated at 4 °C with anti-NgR1 antibody prior to fixation and incubation with labeled secondary antibodies. *vect*, vector. *C*, shown is the binding of AP or AP-NgR1 ligands to COS-7 cells expressing different NgR1 mutants as indicated. *Ng33*, AP fusion protein of the N-terminal 33 residues of Nogo-66 (*Ng66*). The concentrations of ligands applied were as follows: AP, 30 nM; AP-Nogo-66, 5 nM; AP-Nogo-33, 10 nM; AP-Y4C, 10 nM; AP-Y4C66, 0.5 nM; AP-Lingo-1, 10 nM; AP-OMgp, 10 nM; and AP-MAG, 30 nM. These concentrations are close to the binding K_d of these proteins for NgR1, so any decrease in K_d is reflected in staining intensity. *D*, AP ligand binding to NgR1 mutants was quantitated and is expressed as a percentage of binding to wild-type (*WT*) NgR1.

NgR family members (25). Here, we found that RTN2 and RTN3 interact with NgR1. Because of the high sequence similarity between RTN-66 regions, they very likely interact with the same site in NgR1. We localized this binding site to the center of the concave side of the LRR domain by systematic mutagenesis. The several amino acid changes between NgR1 and NgR2 and NgR3 in this core binding region are likely to explain the specificity of this interaction. Previously, we showed that the amino-terminal half (*underlined* in Fig. 1*W*) of Nogo-66 are critical for receptor binding (15). Analysis of different RTN-66 regions suggested that the amino acid changes in RTN1 (shown in *red* in Fig. 1*W*) could account for the loss of its affinity for NgR1. Amino acids 36–41 in RTN-66 regions show considerable sequence diversity. This C-terminal part of Nogo-66 is instrumental for activating NgR1 downstream signaling (15). As our previous results showed that glutathione *S*-transferase-fused RTN1-66 and RTN3-66 recombinant proteins do not cause growth cone collapse (4), other RTNs could thus function as NgR1 antagonists, blocking Nogo-66-induced NgR1 activation. However, as ~95% of these glutathione *S*-transferase proteins are misfolded and in inclusion bodies, it is plausible that the remaining protein fraction might be inactive as well. Although no *Rtn1* or *Rtn3* mRNA expression has been detected in the optic nerve (4), expression of other RTNs in spinal cord white matter had not been previously analyzed. We found that the *Rtn3* mRNA transcript containing the 66-amino acid loop region is expressed in spinal cord white matter at levels similar to those of Nogo-A. Previous studies showed that different splice forms of endogenous RTN4 interact with each other (34) and that Nogo-B interacts with RTN3 (35). As the Nogo-B/RTN3 interaction is mediated by the RHD (35), Nogo-A and RTN3 may also form complexes in glial cells. The stoichiometry of RTN3·RTN4 complexes might determine their function.

Most of Nogo-A is localized to the endoplasmic reticulum, where it serves essential functions in a wide variety of cells (29). Accumulating evidence shows that at least a fraction of oligodendrocyte plasma membrane Nogo-A is in a conformation in which the N terminus of the protein faces the extracellular milieu (3, 34). Recently, we demonstrated that a second Nogo-A-specific

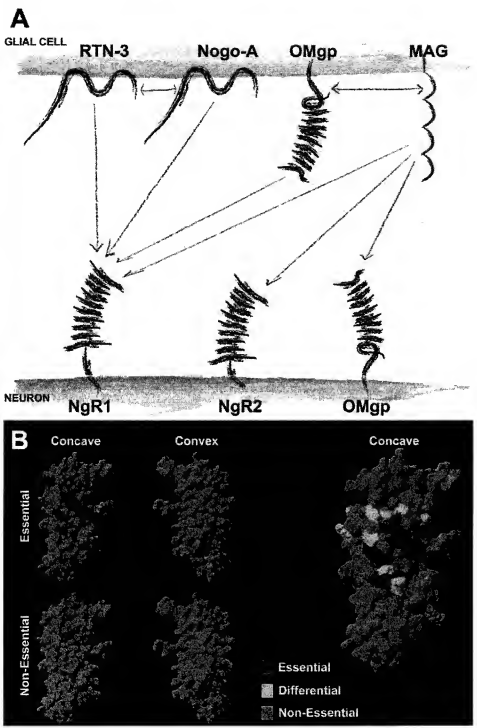

FIGURE 7. **Mapping of ligand-binding sites in NgR1 and summary of the observed interactions.** *A*, summary of the observed interactions between ligands expressed in the oligodendrocytes and their neuronal receptors. *Bidirectional arrows* denote potential interactions in *cis* between proteins presented on the oligodendrocyte plasma membrane. *B*, summary of the ability of 74 Ala-substituted human NgR1 mutants to bind Nogo-66, MAG, and OMgp ligands. Residues required for the binding of all three ligands (*red*) or some ligands but not others (*yellow*) and those not required for ligand binding (*blue*) are highlighted. This illustration was made using Swiss-PdbViewer software.

domain (Nogo-A-24, human Nogo-A amino acids 995–1018) immediately N-terminal to the first hydrophobic segment has separate high affinity for NgR1 (31). Here, we have reported that the C terminus following the second C-terminal hydrophobic region in the RHD also interacts with NgR1 with high affinity. It is possible that, like several other proteins, Nogo-A could adapt multiple conformations to encompass different functions or to target the protein into different cellular compartments (for review, see Ref. 36). The C-terminal end of Nogo-A possesses an endoplasmic reticulum-targeting sequence, *-KXKXX*. This pentapeptide has to be cytosolic to be recognized. Thus, it is possible that the population of Nogo-A protein molecules that present their C termini extracellularly or on the luminal side of the endoplasmic reticulum might be enriched on the plasma membrane.

As the three Nogo-A segments that bind to NgR1 are closely connected to each other in a single polypeptide chain, it is plausible that they cannot interact with several distant sites in a single NgR1 molecule. Interestingly, we noted that the binding sites of Nogo-66, Nogo-Y4C, and Nogo-C39 on NgR1 overlap. It is feasible that these fragments might not interact simultaneously with one NgR1 monomer, but that tripartite NgR1 ligand would engage NgR1 clustering. The extracellular domain of NgR1 has significant affinity for surface-bound NgR1, and given the presumably high local concentration of glycosylphosphatidylinositol-anchored NgR1 in lipid rafts, receptor clustering could be facilitated by this basal level homophilic adhesion (33). Consistent with the receptor clustering model, clustering of MAG and Nogo-66 has been shown to increase their potency to activate NgR1 signaling and downstream RhoA activation (37). Previously, we noticed that fusion of Nogo-A-24 (which is able to bind but not activate NgR1) to the NEP-(1–32) antagonist peptide creates a potent agonist peptide (31). This result also raised the possibility that bivalent or multivalent interactions of ligands with NgR1 are critical for its activation.

The observed very high affinity interaction between OMgp and MAG suggests a model in which a ternary complex consisting of OMgp, MAG, and NgR1 could regulate

TABLE 1

Summary of the ligand binding properties of the NgR1 mutants

Ala-substituted NgR1 mutants were tested for their binding to AP-Nogo-66, AP-Y4C, AP-Y4C66, AP-Nogo-C39, AP-Lingo-1, AP-OMgp, and AP-MAG, and they fall into three categories: 1) mutants that lose binding to all NgR1 ligands, 2) mutants that still maintain binding to all NgR1 ligands, and 3) differential binding mutants that bind some ligands but lose binding to other ligands. The D259N mutant is an asparagine substitution to mimic a human polymorphism.

Residues		
No binding	Binding to all ligands	Differential binding
163	61	82
82, 179	92	108
133, 136	122	139
158, 160	127	210
182, 186	131	78, 81
232, 234	138	87, 89
67, 68, 71	151	89, 90
111, 113, 114	176	95, 97
114, 117, 163	179	108, 131
182, 186, 210	227	256, 259
210, 232, 234	250	36, 38, 61
67, 68, 95, 97	D259N	61, 108, 131
87, 89, 133, 136	36, 38	95, 97, 122
182, 186, 158, 160	63, 65	114, 117, 139
111, 113, 114, 138	114, 117	117, 119, 120
117, 119, 120, 139	127, 151	216, 218, 220
95, 97, 188, 189, 191, 192	127, 176	220, 223, 224
202, 205, 227, 250, 277, 279	143, 144	237, 256, 259
95, 97, 117, 119, 120, 188, 189	189, 191	256, 259, 284
	196, 199	237, 256, 284
	202, 205	63, 65, 87, 89
	267, 269	196, 199, 220, 223, 224
	277, 279	211, 213, 237, 256, 259, 284
	189, 191, 237	189, 191, 211, 213, 237, 256, 259, 284
	189, 191, 284	
	202, 205, 227	
	202, 205, 250	
	296, 297, 300	
	171, 172, 175, 176	
	292, 296, 297, 300	
	171, 172, 175, 176, 196, 199	

TABLE 2

List of NgR1 mutants that show differential binding to NgR1 ligands

The binding of Ala-substituted NgR1 mutants to NgR1 ligands was compared with that of wild-type NgR1, and the levels of binding were categorized as follows: wild-type level (++), weaker than the wild-type level (+), trace binding (tr), no binding (−), and not determined (ND).

Residues	Nogo-66	Nogo-Y4C	Nogo-C39	Nogo-Y4C-66	Lingo-1	OMgp	MAG	Anti-NgR1
Wild-type	++	++	++	++	++	++	++	++
82	++	++	++	++	+	+	−	++
108	++	++	++	++	tr	+	−	++
139	+	+	+	+	−	tr	−	++
210	+	+	+	+	−	−	−	+
78, 81	++	++	++	++	tr	++	ND	++
87, 89	++	++	++	++	−	+	+	++
89, 90	+	+	+	+	−	−	−	++
95, 97	+	+	+	+	+	tr	tr	++
108, 131	+	+	+	+	−	+	tr	++
256, 259	++	++	++	++	++	+	−	++
36, 38, 61	+	+	+	++	tr	+	tr	++
61, 108, 131	+	+	+	+	−	−	−	++
95, 97, 122	+	+	+	+	−	tr	tr	++
114, 117, 139	+	+	+	+	−	−	−	++
117, 119, 120	++	++	++	++	tr	tr	−	++
216, 218, 220	++	++	++	++	+	+	tr	++
220, 223, 224	+	+	+	+	−	−	tr	++
237, 256, 259	tr	tr	tr	+	+	tr	−	++
256, 259, 284	+	+	+	++	++	+	−	++
63, 65, 87, 89	++	++	++	++	−	+	−	++
237, 256, 284	++	++	++	++	++	+	−	++
211, 213, 237, 256, 259, 284	−	−	−	−	++	−	−	++
189, 191, 211, 213, 237, 256, 259, 284	−	−	−	−	++	−	ND	++

specific aspects of oligodendrocyte/neuron interactions. At least in some cases, OMgp could also serve as a high affinity neuronal ligand for MAG. This is supported by a report that OMgp is expressed at low levels in oligodendrocytes, whereas neuronal expression of OMgp, as detected by immunohistochemistry and *in situ* hybridization, is prominent (38). Interestingly, the reported neuronal expression pattern of OMgp overlaps (e.g. in layer V of the cerebral cortex and pyramidal cells of the hippocampus) with that of NgR1. Thus, OMgp could contribute to MAG binding in these cells, and farther downstream signaling might depend on the formation of a ternary complex of MAG, OMgp, and NgR1. Neuronal signaling triggered by OMgp/MAG interaction may also be independent of NgR1.

NgR Family/Ligand Interactions

Because the NgR1 structure is now defined (10, 11), we probed its surface for ligand-binding sites using Ala substitutions. There appears to be a binding domain located in the central region on the concave side of the NgR1 LRR domain required by Nogo-A-24, Nogo-66, Nogo-C39, MAG, and OMgp ligands. In addition, different ligands require particular residues surrounding this central site. Because all ligands require surface residues centered on the midportion of the concave face of NgR1, their mechanism for activating NgR1 signaling may be similar. Similar to the case with internalin-E-cadherin (39) and glycoprotein Ibα-von Willebrand factor (40) complexes, the concave side of the receptor serves as a ligand-docking site. Previous work had been divided as to whether binding sites for Nogo-66 and MAG are separate or overlapping. Using the NEP-(1–40) antagonist of Nogo-66, we did not observe inhibition of MAG interactions with NgR1 (8). With a sterically encumbered AP-Nogo-66 ligand, some competition with MAG-Fc binding to NgR1 was detected. Our findings are consistent with partial competition between ligands.

Because NgR1 is considered a target for the development of axonal regeneration therapeutics (41), the definition of this central binding domain shared by multiple ligands may facilitate the design and development of small molecule therapeutics blocking all NgR1 ligands. In contrast, if each ligand had been found to require completely separate residues for binding with high affinity, then the challenge of developing blockers of all myelin protein action at NgR1 would be significantly higher.

Lingo-1 has been reported as a component of a signal-transducing NgR1 complex (30). It is notable that the residues required for Lingo-1 binding to NgR1 are very similar to those for ligands MAG and OMgp. Because Lingo-1 in also expressed by oligodendrocytes, the binding analysis suggested that it might act as a ligand for NgR1.

The systematic mapping of all interactions between myelin inhibitory ligands and related molecules and NgR family members gives us better insight into the possible redundancy in signaling pathways and the specificity of previously described interactions. Novel ligand/receptor interactions were elucidated, so future studies can characterize them in greater functional detail. The identification of a central ligand-binding domain holds the promise that general NgR1 antagonists may be created to possibly promote axonal regeneration after central nervous system injury.

Acknowledgments—We thank Dr. S. Mi (Biogen Idec) for the AP-Lingo-1 and AP-OMgp constructs, Dr. J. G. Flanagan for the pAPtag5 plasmid, and Dr. Eric Schmidt for kindly providing data presented in supplemental Fig. 2. We thank Dr. Noam Harel for critical comments on the manuscript.

REFERENCES

1. Yiu, G., and He, Z. (2006) *Nat. Rev. Neurosci.* **7**, 617–627
2. Liu, B. P., Cafferty, W. B., Budel, S. O., and Strittmatter, S. M. (2006) *Philos. Trans. R. Soc. Lond. B Biol. Sci.* **361**, 1593–1610
3. Oertle, T., van der Haar, M. E., Bandtlow, C. E., Robeva, A., Burfeind, P., Buss, A., Huber, A. B., Simonen, M., Schnell, L., Brosamle, C., Kaupmann, K., Vallon, R., and Schwab, M. E. (2003) *J. Neurosci.* **23**, 5393–5406
4. GrandPre, T., Nakamura, F., Vartanian, T., and Strittmatter, S. M. (2000) *Nature* **403**, 439–444
5. Oertle, T., Klinger, M., Stuermer, C. A., and Schwab, M. E. (2003) *FASEB J.* **17**, 1238–1247
6. Fournier, A. E., GrandPre, T., and Strittmatter, S. M. (2001) *Nature* **409**, 341–346
7. Domeniconi, M., Cao, Z., Spencer, T., Sivasankaran, R., Wang, K., Nikulina, E., Kimura, N., Cai, H., Deng, K., Gao, Y., He, Z., and Filbin, M. (2002) *Neuron* **35**, 283–290
8. Liu, B. P., Fournier, A., GrandPre, T., and Strittmatter, S. M. (2002) *Science* **297**, 1190–1193
9. Wang, K. C., Koprivica, V., Kim, J. A., Sivasankaran, R., Guo, Y., Neve, R. L., and He, Z. (2002) *Nature* **417**, 941–944
10. He, X. L., Bazan, J. F., McDermott, G., Park, J. B., Wang, K., Tessier-Lavigne, M., He, Z., and Garcia, K. C. (2003) *Neuron* **38**, 177–185
11. Barton, W. A., Liu, B. P., Tzvetkova, D., Jeffrey, P. D., Fournier, A. E., Sah, D., Cate, R., Strittmatter, S. M., and Nikolov, D. B. (2003) *EMBO J.* **22**, 3291–3302
12. Schnell, L., and Schwab, M. E. (1990) *Nature* **343**, 269–272
13. Bregman, B. S., Kunkel-Bagden, E., Schnell, L., Dai, H. N., Gao, D., and Schwab, M. E. (1995) *Nature* **378**, 498–501
14. Wiessner, C., Bareyre, F. M., Allegrini, P. R., Mir, A. K., Frentzel, S., Zurini, M., Schnell, L., Oertle, T., and Schwab, M. E. (2003) *J. Cereb. Blood Flow Metab.* **23**, 154–165
15. GrandPre, T., Li, S., and Strittmatter, S. M. (2002) *Nature* **417**, 547–551
16. Lee, J. K., Kim, J. E., Sivula, M., and Strittmatter, S. M. (2004) *J. Neurosci.* **24**, 6209–6217
17. Li, S., and Strittmatter, S. M. (2003) *J. Neurosci.* **23**, 4219–4227
18. Wang, X., Baughman, K. W., Basso, D. M., and Strittmatter, S. M. (2006) *Ann. Neurol.* **60**, 540–549
19. Li, S., Liu, B. P., Budel, S., Li, M., Ji, B., Walus, L., Li, W., Jirik, A., Rabacchi, S., Choi, E., Worley, D., Sah, D. W., Pepinsky, B., Lee, D., Relton, J., and Strittmatter, S. M. (2004) *J. Neurosci.* **24**, 10511–10520
20. Simonen, M., Pedersen, V., Weinmann, O., Schnell, L., Buss, A., Ledermann, B., Christ, F., Sansig, G., van der Putten, H., and Schwab, M. E. (2003) *Neuron* **38**, 201–211
21. Zheng, B., Ho, C., Li, S., Keirstead, H., Steward, O., and Tessier-Lavigne, M. (2003) *Neuron* **38**, 213–224
22. Kim, J. E., Li, S., GrandPre, T., Qiu, D., and Strittmatter, S. M. (2003) *Neuron* **38**, 187–199
23. Zheng, B., Atwal, J., Ho, C., Case, L., He, X. L., Garcia, K. C., Steward, O., and Tessier-Lavigne, M. (2005) *Proc. Natl. Acad. Sci. U.S.A.* **102**, 1205–1210
24. Kim, J. E., Liu, B. P., Park, J. H., and Strittmatter, S. M. (2004) *Neuron* **44**, 439–451
25. Laurén, J., Airaksinen, M. S., Saarma, M., and Timmusk, T. (2003) *Mol. Cell. Neurosci.* **24**, 581–594
26. Pignot, V., Hein, A. E., Barske, C., Wiessner, C., Walmsley, A. R., Kaupmann, K., Mayeur, H., Sommer, B., Mir, A. K., and Frentzel, S. (2003) *J. Neurochem.* **85**, 717–728
27. Venkatesh, K., Chivatakarn, O., Lee, H., Joshi, P. S., Kantor, D. B., Newman, B. A., Mage, R., Rader, C., and Giger, R. J. (2005) *J. Neurosci.* **25**, 808–822
28. Yan, R., Shi, Q., Hu, X., and Zhou, X. (2006) *Cell. Mol. Life Sci.* **63**, 877–889
29. Voeltz, G. K., Prinz, W. A., Shibata, Y., Rist, J. M., and Rapoport, T. A. (2006) *Cell* **124**, 573–586
30. Mi, S., Lee, X., Shao, Z., Thill, G., Ji, B., Relton, J., Levesque, M., Allaire, N., Perrin, S., Sands, B., Crowell, T., Cate, R. L., McCoy, J. M., and Pepinsky, R. B. (2004) *Nat. Neurosci.* **7**, 221–228
31. Hu, F., Liu, B. P., Budel, S., Liao, J., Chin, J., Fournier, A., and Strittmatter, S. M. (2005) *J. Neurosci.* **25**, 5298–5304
32. Flanagan, J. G., Cheng, H. J., Feldheim, D. A., Hattori, M., Lu, Q., and Vanderhaeghen, P. (2000) *Methods Enzymol.* **327**, 19–35
33. Fournier, A. E., Gould, G. C., Liu, B. P., and Strittmatter, S. M. (2002) *J. Neurosci.* **22**, 8876–8883
34. Dodd, D. A., Niederoest, B., Bloechlinger, S., Dupuis, L., Loeffler, J. P., and Schwab, M. E. (2005) *J. Biol. Chem.* **280**, 12494–12502
35. Qi, B., Qi, Y., Watari, A., Yoshioka, N., Inoue, H., Minemoto, Y., Yamashita, K., Sasagawa, T., and Yutsudo, M. (2003) *J. Cell. Physiol.* **196**,

312–318
36. Levy, D. (1996) *Essays Biochem.* **31,** 49–60
37. Niederost, B., Oertle, T., Fritsche, J., McKinney, R. A., and Bandtlow, C. E. (2002) *J. Neurosci.* **22,** 10368–10376
38. Habib, A. A., Marton, L. S., Allwardt, B., Gulcher, J. R., Mikol, D. D., Hognason, T., Chattopadhyay, N., and Stefansson, K. (1998) *J. Neurochem.* **70,** 1704–1711
39. Schubert, W. D., Urbanke, C., Ziehm, T., Beier, V., Machner, M. P., Domann, E., Wehland, J., Chakraborty, T., and Heinz, D. W. (2002) *Cell* **111,** 825–836
40. Huizinga, E. G., Tsuji, S., Romijn, R. A., Schiphorst, M. E., de Groot, P. G., Sixma, J. J., and Gros, P. (2002) *Science* **297,** 1176–1179
41. Lee, D. H., Strittmatter, S. M., and Sah, D. W. (2003) *Nat. Rev. Drug Discov.* **2,** 872–878